HEAD LOSS THROUGH FIBROUS DEBRIS BED WITH DIFFERENT TYPES OF PERFORATED STRAINERS

A Thesis

by

SUHAEB SABAH ABDULSATTAR

Submitted to the Office of Graduate and Professional Studies of
Texas A&M University
in partial fulfillment of the requirements for the degree of

MASTER OF SCIENCE

Chair of Committee,	Yassin A. Hassan
Committee Members,	William H. Marlow
	Victor M. Ugaz
Head of Department,	Yassin A. Hassan

May 2014

Major Subject: Nuclear Engineering

ABSTRACT

Safety related issues in Nuclear Power Plants (NPPs) have always been of concern, especially those issues that are related to Light Water Reactors (LWRs) and their Design Basis Accidents (DBA). One of the ongoing issues that has been extensively studied is the Generic Safety Issue GSI-191, which is dedicated to study and resolve the issues that arise after a Loss-Of-Coolant-Accident (LOCA). Fibrous debris produced during the blow-down phase of Loss-of-Coolant Accidents is transported into the sump and becomes an important cause of head loss through the sump strainer, affecting the Emergency Core Cooling System (ECCS) performance. This study was dedicated to measure the pressure drop across randomly accumulated debris bed on the sump strainer along with measuring the debris bed thickness. Two different types of strainers were installed vertically, one at a time, in a horizontal flow loop and the debris bed thickness was measured during the bed build up process and after reaching steady state. Fifteen tests were conducted to determine the head loss difference between the two strainers and to study the characteristics of the debris bed accumulated on each strainer. The results from this experimental study were compared based on the approaching velocity, debris bed thickness, and strainer type. A realistic permeability model for the NUKON fiber glass insulation material was suggested, to be utilized in related applications, the suggested head loss model was compared to other head loss models developed in previous studies. The permeability model was developed from experimental data acquired from approaching velocities in the viscous region. There was

no significant head loss difference between the two strainers for the minimum and intermediate range. Based on the experimental data, the head loss difference between the two strainers for the maximum range was about four times higher than the calculated head loss. The flow rate measurement uncertainty was main reason for the difference in the maximum range. There is a probability that the debris bypass could be different between the two strainers, thus, a debris bypass study is required to further investigate this difference.

ACKNOWLEDGEMENTS

The author wishes to acknowledge and thank several people. I would like to thank my advisor, Dr. Hassan, for his exemplary guidance and constant encouragement throughout the course of this thesis. I would like to thank my colleague, Saya Lee, for his technical support and discussion. Also, I would like to thank my colleague and classmate, Matthew Kappes, for his help with English grammar and Mathematica software. Finally, I would like to thank my family for their love and support.

NOMENCLATURE

BWR	Boiling Water Reactor
DBA	Design Basis Accident
DEBG	Double Ended Guillotine Break
ECCS	Emergency Core Cooling System
FPS	Frame per Second
GL	Generic Letter
GSI	Generic Safety Issue
LBLOCA	Large Break Loss of Coolant Accident
LOCA	Loss of Coolant Accident
LWR	Light Water Reactor
MBLOCA	Medium Break Loss of Coolant Accident
MSDS	Material Safety Data Sheet
NEI	Nuclear Energy Institute
NIST	National Institute of Standards and Technology
NPP	Nuclear Power Plants
NPSH	Net Positive Suction Head
NRC	Nuclear Regulatory Commission
PCI	Performance Contracting Incorporation
PSID	Pound per Square Inch Differential
PVC	Polyvinyl Chloride

PWR	Pressurized Water Reactor
RCS	Reactor Cooling System
RHR	Residual Heat Removal
RWST	Refueling Water Storage Tank
SBLOCA	Small Break Loss of Coolant Accident
STP	South Texas Project
ZOI	Zone of Influence

TABLE OF CONTENTS

Page

LIST OF FIGURES

Page

LIST OF TABLES

Page

1. INTRODUCTION

Safety related issues in Nuclear Power Plants (NPPs) have always been of concern, whether for the public or for the nuclear industry, especially those issues that are related to Light Water Reactors (LWRs). There are currently 100 NPPs licensed to operate in the United States: 65 Pressurized Water Reactors (PWRs) and 35 Boiling Water Reactors (BWRs) [1]. One of the ongoing issues that has been extensively studied is the Generic Safety Issue GSI-191, "Assessment of Debris Accumulation on PWR Sump Performance," [2]. This study started in 1979 when the U.S. Nuclear Regulatory Commission (NRC) established Unresolved Safety Issue USI A-43, "Containment Emergency Sump Performance," which is dedicated to study and resolve the issues that arise after a Loss-Of-Coolant-Accident (LOCA), in particular, the availability of adequate recirculation coolant water and the performance of the containment sump of PWRs, this safety issue can also be applied to the Residual Heat Removal System (RHR) of BWRs [3]. On July 28, 1992 the suction strainer of the Emergency Core Cooling System (ECCS) pump at Unit 2 of the Swedish BWR Barsebäk was partially clogged due to a containment spray accident. In this accident, larger quantities of the fibrous debris reached the strainer than had been anticipated by the USI A-43 study [4]. Two more related events occurred in 1993 at Perry Unit 1, the first event took place on January 16 when the ECCS strainers were plugged by debris transported from the suppression pool, the second event occurred when the ECCS strainers were plugged by debris from the suppression pool on April 14, but this time the debris originally came

from the ventilation filters after they fell into the suppression pool. During both of these events, the strainers of the ECCS were damaged due to the excessive differential pressure created by the debris accumulation on the strainers [4]. The last related event occurred on September 11, 1995. This event took place at Limerick Unit 1due to debris accumulation on the suction strainers of the ECCS pump. The NRC issued several letters requesting different modifications for the LWRs licensing to minimize the potential of ECCS suction strainer clogging due to debris transportation and accumulation following a LOCA [5][6]. This experimental study was initiated in response to GSI-191, it is dedicated to investigate the head loss across the debris bed due to the accumulation of debris on the sump strainer using specific type of insulation material, called NUKON^{TM}, with two different types of strainers to simulate both South Texas Project (STP) NPP sump strainer and Vogtle Electric Generation Plant, also known as Plant Vogtle, sump strainer.

2. LITERATURE REVIEW

A considerable number of models have been developed to study the flow resistance through a porous media based on Darcy's law as shown in Equation 2.1,

$$\frac{\Delta P}{\Delta L} = \frac{\mu U}{K} \tag{2.1}$$

where, P is the pressure, L is the thickness of the porous bed, μ is the dynamic viscosity, U is the approaching velocity, and K is the permeability. This relationship only holds when the viscous force is dominant. In order for that to happen, the flow rate must be very low. Kozeny-Carmen equation, as shown in Equation 2.2, showed good agreement with the experimental data of packed bed,

$$\frac{\Delta P}{\Delta L} = -kS_v^2 \frac{(1-\varepsilon)^2}{\varepsilon^3} \mu U \tag{2.2}$$

where, k is Kozeny constant, S_v is the specific surface area, and ε is the bed porosity, which is smaller than 0.5 for packed bed [7]. The Kozeny constant was developed by Ingmanson et al. [8] and Ergun [9] and modified by Zigler et al. [10]. It can be represented by the modified Davies [11] model, Davies suggested a model for fibrous beds with higher porosity, $0.7 < \varepsilon < 0.99$, using experimental data for fiber filtration with air as shown in Equation 2.3,

$$k = a\frac{\varepsilon^3}{(1-\varepsilon)^{0.5}}[1 + b(1-\varepsilon)^3] \quad 2.3$$

where, *a* and *b* are empirical coefficients with suggested values of a= 4.0 and b = 56. Ingmanson et al. [8] conducted head loss experiments through fiberglass bed and modified Davies model with new coefficients, a = 3.5 and b= 57. Ingmanson et al. used a uniform fibrous bed in their experiment which creates higher pressure drop than the randomly generated debris bed on the sump strainer of the NPP. The U.S. NRC began their analysis in 1996 in order to predict and estimate the loss of the Net Positive Suction Head (NPSH) by establishing GSI-191. In 1995, NUREG/CR-6224[10] estimated the head loss due to the debris bed formation on the sump strainer as a semi-theoretical model of head loss as shown in Equation 2.4,

$$\frac{\Delta P}{\Delta L_0} = \left[3.5S_v^2(1-\varepsilon_m)^{1.5}[1 + 57(1-\varepsilon_m)^3]\mu U + 0.66s_v\frac{(1-\varepsilon_m)}{\varepsilon_m^3}\rho_w U^2\right]\left(\frac{\Delta L_m}{\Delta L_0}\right) \quad 2.4$$

where, L_m is the actual bed thickness, L_0 is the fiber bed theoretical thickness, ε_m is the mixed bed porosity and ρ_w is the water density. Eq. 2.4 consists of two terms: the viscous term and the inertial term, it was developed for earlier strainer designs with higher approaching velocities and smaller surface area, meaning that the Kozeny constant, *k*, need to be reevaluated based on the current strainer design. The debris bed thickness and the porosity of the debris bed were measured to calculate the Kozeny constant from Eq. 2.2. The porosity of the fibrous debris bed, ε, can be calculated from equation 2.5,

$$\varepsilon = 1 - \frac{M_s(t)}{A\, L_{avg}(t)\rho} \qquad 2.5$$

where, A is the surface area of the strainer, ρ is the density of the NUKON, $L_{avg}(t)$ is the average thickness of the debris bed at time t, and $M_s(t)$ is the mass of the debris on the strainer at time t, which can be calculated using pictures of the debris bed and Equation 2.6,

$$M_s(t) = M_0\left[1 - e^{-\frac{AUC_f t}{V_t}}\right] \qquad 2.6$$

where, M_0 is the initial mass of the debris in the tank, A is the surface area of the strainer, C_f is the filtration coefficient and V_t is the volume of the water in the tank,

$$L_{avg}(t) = \frac{1}{N}\sum_{i=1}^{N} L_i \qquad 2.7$$

where, L_i is the thickness of the fibrous debris bed at point P_i, and N is the number of the point along the axial direction of the debris bed. For this experimental study, the average debris bed thickness, L_{avg}, was calculated by taking the average of the bed thickness at 10 points with uniform spacing along the axial direction as it will be explained in later sections.

3. RESEARCH OBJECTIVE AND APPROACH

The objective of this study is to suggest a realistic permeability model for the NUKON fiber glass insulation material, which can be utilized in related applications. This study is dedicated to measuring the pressure drop across randomly accumulated debris bed on the sump strainer along with measuring the debris bed thickness during the bed build up process and after reaching steady state. Two different types of strainers were installed vertically, one at a time, in the horizontal flow loop. These strainers were fabricated to simulate the sump strainers of two different nuclear power plants.

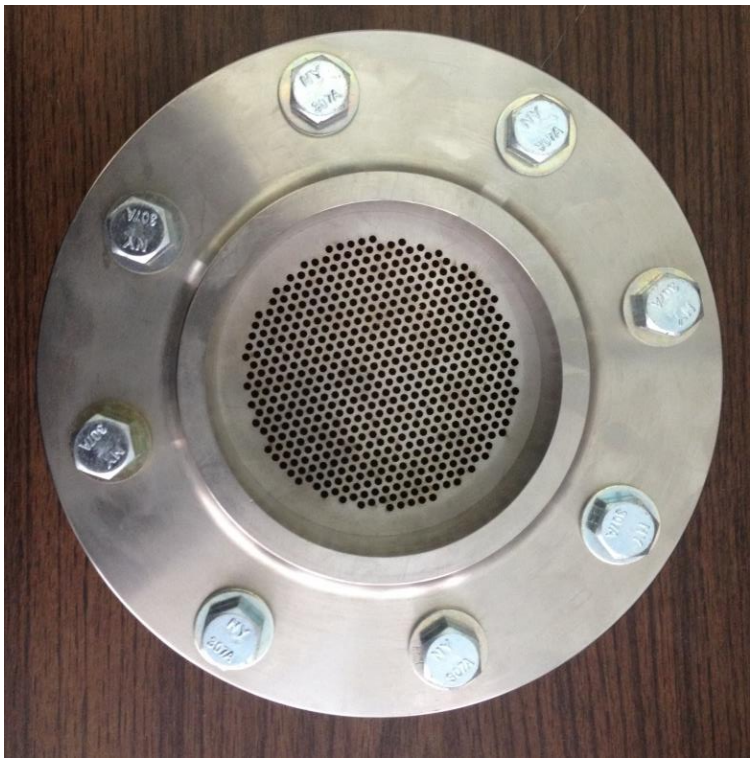

Figure 3.1 Perforated Stainless-Steel Plate

Figure 3.1 shows the first strainer type, a stainless-steel perforated plate, which was fabricated to simulate the South Texas Project (STP) sump strainer [12]. The second strainer type was fabricated to simulate the Vogtle nuclear power plant sum strainer as shown in Figure 3.2.

Figure 3.2 Perforated Stainless-Steel Plate with Embedded Mesh

The above strainer was fabricated with the same characteristics as the STP strainer, the only difference is that stainless-steel wire mesh was welded on the plate to simulate the Vogtle NPP sump strainer. Both of these strainers were fabricated with the same characteristics of an actual PWR sump strainer shown in Table 3.1

Table 3.1 Typical PWR Sump Strainer Characteristics

Plate Thickness	1.56 mm
Pitch	3.96 mm
Hole Diameter	2.42 mm
Wire Mesh Diameter	3.05 mm (Vogtle only)
Mesh Opening Size	10.16 mm (Vogtle only)

A High Definition (HD) Camera was set on a tripod about 50 cm away from the strainer to record the process of the debris bed buildup for the entire experiment time, these videos were used in later analysis by taking pictures at different time intervals within the experiment time to calculate the debris bed thickness at different points on the axial direction parallel to the strainer as will be discussed in section 6.

4. EXPERIMENTAL FACILITY CONDITIONS

The experimental facility was designed and built to simulate the containment sump strainer of a typical PWR as shown in Figure 4.1. Both of the strainers were designed and manufactured to comply with the actual sump strainer characteristics shown in Table 3.1. The perforated plates were manufactured with a surface area of 12.57 in^2 (81.07cm^2) to fit inside a pipe with a diameter of 4 in (10.16 cm).

Figure 4.1 PWR Sump Strainers (http://www.pciesg.com/sure-flow_gallery.php)

The sump strainer, depending on the break size, will be fully submerged in water, after LOCA. The debris rustling from the blow-down is transported to the sump and filtered through the strainers and, then, the debris bed accumulated on the sump strainer as it's being sucked by the pump as shown in Figure 4.2.

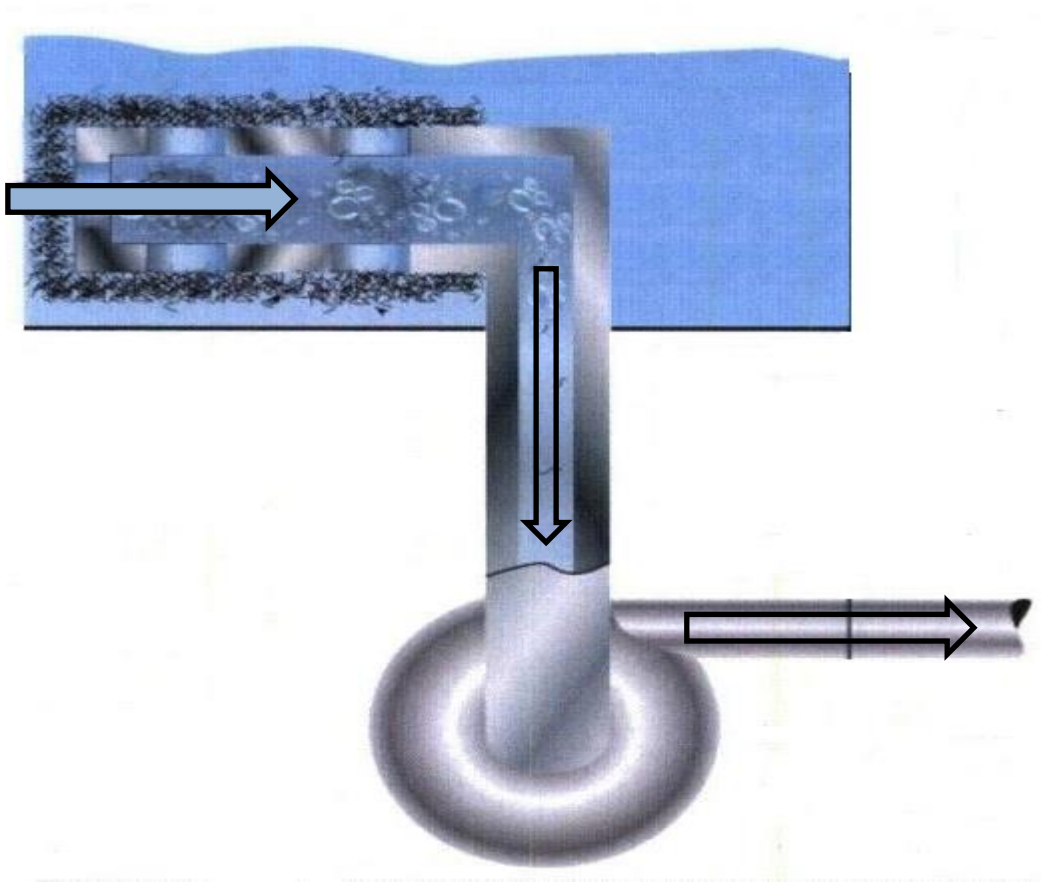

Figure 4.2 Illustration of the Containment Sump after LOCA

(Partially taken from CASA Grande Analysis [13])

4.1 Experimental Conditions

The experimental conditions were determined based on the conditions of a typical PWR sump strainer defined in Table 4.1.

Table 4.1 PWR Sump Strainers Condition

Strainer nominal flow rate	7020 GPM (26573.58 l/min)
Strainer surface area	1818.5 ft^2 (168.94 m^2)
Approaching Velocity	0.009 ft./s (0.274 cm/s)
Debris Type	NUKON
Debris Diameter	7.112 μm
Liquid	Tap water

The experimental study used the same approaching velocity as for the actual system, because it was important to use the same debris characteristics (i.e. type and diameter) of the actual system. The debris characteristics were kept the same, because Reynolds number (Re) in porous media, also called modified Reynolds number (Re_m), depends on the particle diameter as shown in equation 4.1,

$$Re_m = \frac{\rho u \, D_N}{\mu(1-\varepsilon)} \qquad 4.1$$

where, ρ is the density of the fluid, U is the approaching velocity, D_N is the diameter of the particle (NUKON).The experimental facility was designed with piping of 4 inch (10.16 cm) in diameter and the flow rate values were calculated based on the actual PWR sump strainer condition taking into consideration the pipe diameter as shown in Table 4.2.

Table 4.2 Experimental Conditions

Strainer nominal flow rate	21.12 GPH (1.33 l/min)
Strainer surface area	0.0873 ft^2 (81.07 cm^2)
Approaching Velocity	0.009 ft./s (0.274 cm/s)
Debris Type	NUKON
Debris Diameter	7.112 μm
Liquid	Tap water

The sump strainer approaching velocity of the system (0.274 cm/s) was considered as the nominal approaching velocity, and the experimental study was conducted for higher approaching velocity assuming extreme condition. The pressure drop through the strainer was measured at three different approaching velocities, 0.311 cm/s corresponding to flow rate of 24 GPH (0.02524 l/s), 1.167 cm/s corresponding to flow rate of 90 GPH (0.9464 l/s), and 3.112 cm/s corresponding to a flow rate of 240 GPH (0.25236 l/s) as shown in table 4.3. The free Reynolds Number, not the modified, for each range was calculated using equation 4.2,

$$Re = \frac{\rho u\, D_p}{\mu} \qquad 4.2$$

where, D_p is the diameter of the pipe, which is 4 inch (10.16 cm) for this experimental study.

Table 4.3 Approaching Velocity Range

Approaching Velocity	0.311 cm/s	1.167 cm/s	3.112 cm/s
range	Minimum	Intermediate	Maximum
Reynolds number	355	1334	3560

The quantity of LOCA generated debris depends on the location and the size of the side-wall pipe break. The side-wall pipe break size can be classified into three types, pipe breaks with diameter equal or larger than 6 in. (15.25 cm) are defined as Large Break LOCA (LBLOCA), pipe break with diameter larger than 2 in. (5.08 cm) but smaller than 6 in. (15.25cm) are defined as Medium Brake LOCA (MBLOCA), and finally, pipe break with diameter equal or less than 2 in. (5.08cm) are defined as Small Break LOCA (SBLOCA) [10]. The quantity of LOCA generated debris is calculated based on Zone of Influence (ZOI) deterministic models, the ZOI can be modeled as a sphere for fully offset Double Ended Guillotine Break (DGEB) or as a hemisphere for anything less than a DGEB (i.e. side-wall pipe break), the radius of the sphere depends on the break size and the jet pressure, the ZOI size for the NUKON insulation is equal to 17D (STP calculation), where, D is the diameter of the pipe break [13]. The quantity of

the LOCA generated NUKON debris can reach up to 3,000 ft^3 (84.951 m^3), However, 99.9% of the accident scenarios generate less than 10 ft^3 (0.2832 m^3) [13]. The pool water volume is based on the volume of the water in the reactor containment, which comes from the Refueling Water Storage Tank (RWST) and Reactor Coolant System (RCS), the volume of water for LBLOCA is 69,263 ft^3 (1960.545 m^3)[13]. The NUKON concentration (volume %) in the reactor containment can be calculated, assuming LBLOCA, using Equation 4.3,

$$C_N = \frac{V_N}{V_W}\ 100\% \qquad 4.3$$

where, C_N is the concentration of the NUKON per volume, V_N is the volume of the NUKON and V_W is the volume of the water in the reactor containment. Based on these values the concentration of the NUKON was 0.0144 (vol. %.). The water level in the experiment facility tank was set to 20 inch (50.8 cm) making the volume of the water equal to 6.667 ft^3 (0.1888 m^3). The debris quantity in the system was calculated based on the water volume of the experimental system using the same debris concentration in the actual PWR pool. It was determined that the volume of the debris for the experimental system should be equal 0.0964 ft^3 (0.00273 m^3). The density of the NUKON debris particle was specified to be equal to 2.88 g/cm^3 in the (NURE/CR-6224), however, it was specified to be 2.5 g/cm^3 according to the NUKON insulation Material Safety Data Sheet (MSDS)[10][14]. This experimental study is focused on the wall-side break, rather than DEGB, the ZOI was assumed to be of a hemispherical shape and 100% of the debris affected by the blow-down is of the NUKON type. The amount

of the NUKON debris was calculated to be between 34.1 g and 39.6 g, the amount of the NUKON debris was conventional to be equal to 40g assuming extreme event. A summary of all the assumption made for the purpose of this experimental study are shown in Table 4.4.

Table 4.4 Summary of the Experimental Conditions

Parameter	Condition
Break Size	6 in. (15.25 cm) LBLOCA
ZOI	Hemispherical
Total Water Volume	6.667 ft^3 (0.1888 m^3)
Water Type	Tap water
Debris Type	NUKON
Debris Diameter	7.112 μm
Debris Volume	0.0964 ft^3 (0.00273 m^3).
Debris Mass	40 g
Strainer Surface Area	0.0873 ft^2 (81.07 cm^2)
Minimum Approaching Velocity	0.311 cm/s
Intermediate Approaching Velocity	1.167 cm/s
Maximum Approaching Velocity	3.112 cm/s
Test temperature	24±3º C

4.2 Experimental Facility Description

An experimental facility was assembled for the purpose of measuring the pressure drop generated by the debris bed on the strainer and the debris bed thickness at any given time. A stainless-steel perforated plate was installed vertically in a horizontal flow loop consisting of a transparent Acrylic water tank, transparent polycarbonate piping, and Polyvinyl Chloride (PVC) piping. The perforated strainer was installed 14 in (35.56 cm) away from the outlet of the tank using polycarbonate piping with a diameter of 4 in (10.16 cm); polycarbonate piping was also used between the strainer and the inlet of the rotameters. The polycarbonate piping was attached to both sides of the strainer via two flanges that were designed for this purpose. The transparent nature of the polycarbonate piping, on both sides of the strainer, was in favor of visual observation of the debris build up process during the experiment run time and after reaching steady state. The piping diameter was reduced via a pipe reducer from 4 inch (10.16 cm) to 1 inch (2.54 cm) and connected to the rotameters inlet. The rotameters outlet was connected to the recirculation pump suction inlet via a high-pressure flexible tubing to eliminate the effect of the pump vibration on the pressure measurement. Finally, the pump outlet was connected to a gate valve, to control the pump flow more efficiently, which is connected to the water tank inlet using PVC piping with a diameter of 1 in (2.54 cm). The main components of the experimental facility are shown in Figure 4.3 and defined in Table 4.5.

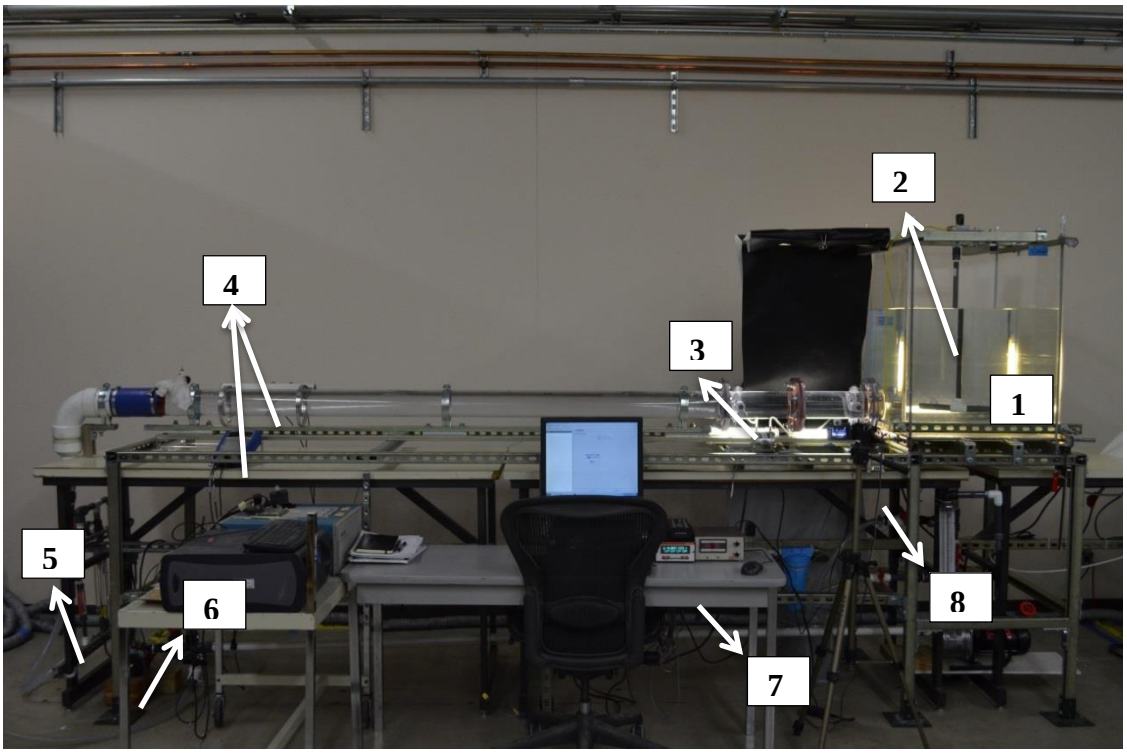

Figure 4.3 Experimental Facility System

Table 4.5 Experimental Facility Components

Number	Components	Number	Components
1	Water Tank	5	Flowmeters Assembly
2	Mixing propeller	6	Circulation Pump
3	Pressure Transducer	7	Data Acquisition
4	Ultra Sonic Flow Meter	8	HD Camcorder

4.2.1 Water Tank

The water tank is made of Acrylic plates with 24 inch (60 .96 cm) in width, 24 inch (60 .96 cm) in length, and 30 inch (76.2 cm) in height. The transparent nature of the tank material allows visual observation through the walls, during the experiment run time, to make sure that the debris are distributed uniformly inside the tanks and to adjust the water level accurately before running the experiment. The inlet of is located at the bottom of the tank, at the center, with diameter of 1 in (2.54 cm), whereas the outlet is located on the side, 2 in (5.08 cm) away from the bottom plate, with diameter of 4 in (10.16 cm) as shown in Figure 4.4.

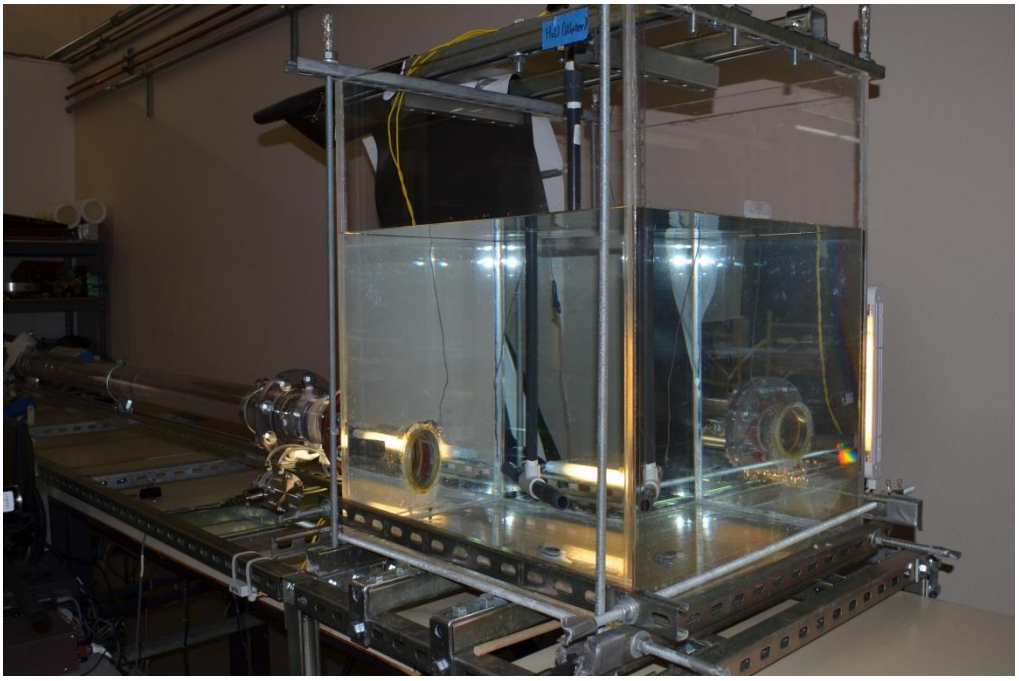

Figure 4.4 Acrylic Water Tank

4.2.2 Mixing Propeller

The mixing propeller is made of three PVC pipes with an otter diameter (OD) of 0.75 in (1.905 cm) for the body and 1 in (2.54cm) for the arms forming a T-shaped mixer as shown in Figure 4.5. The main reason behind installing the mixing propeller was to agitate the NUKON debris inside the tank during the experiment. It was observed that some of the debris were caught on the mixing propeller arms during the stirring process, especially during the first hour of the experiment where the debris concentration in the tank at its maximum values. In order to overcome this issue, a time-adjusted relay [15], as shown in Figure 4.6, was installed to switch the direction of rotation at any desired time interval. For the purpose of this experimental study, the relay was adjusted to alternate the direction of rotation every 5 minutes.

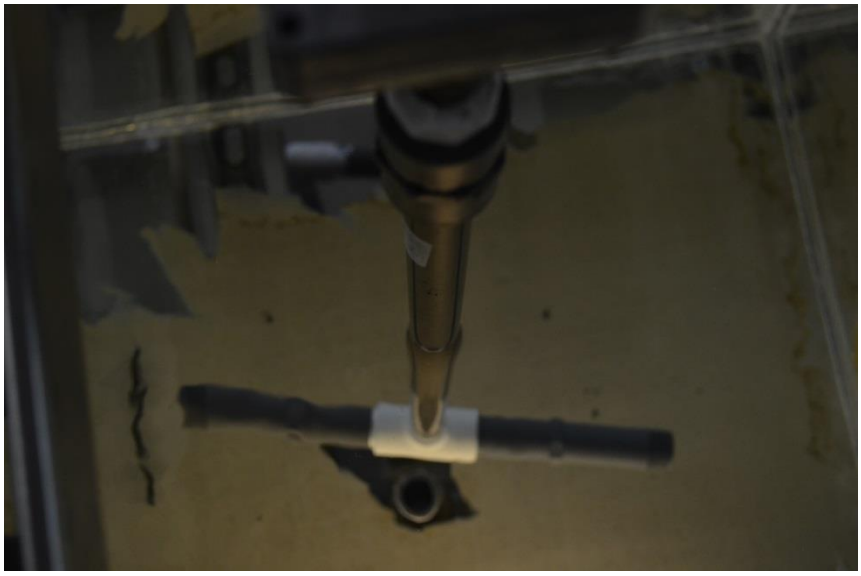

Figure 4.5 T-Shaped Mixing Propeller

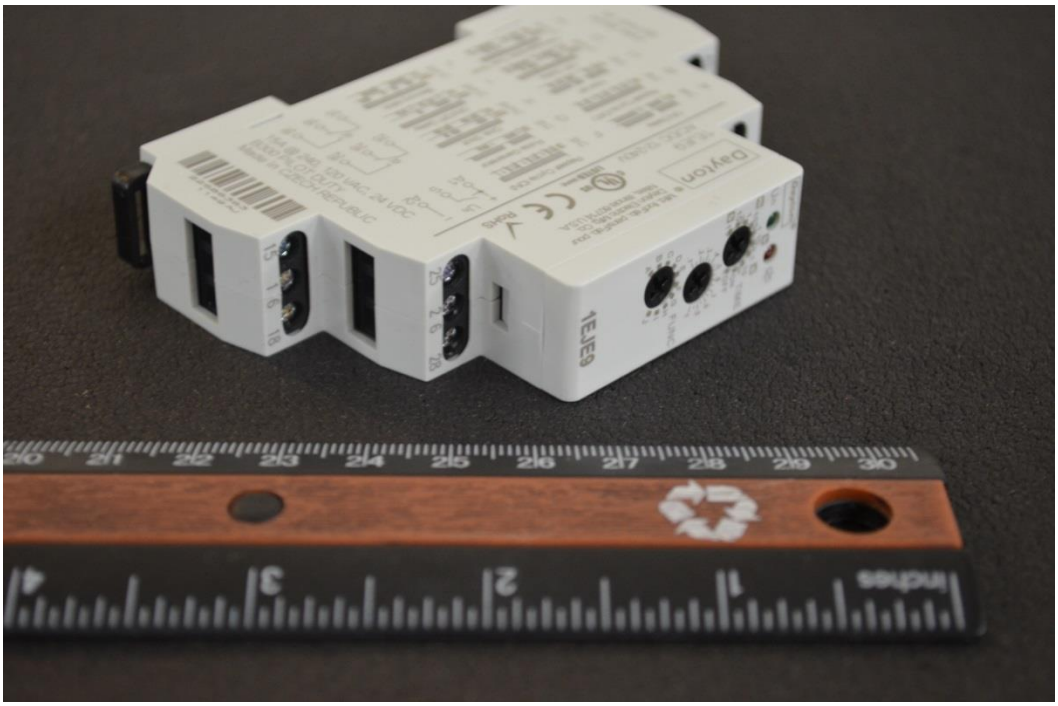

Figure 4.6 Dayton® Time Delay Realy (Model# 1EJE9)

It was argued that the rotation of the mixing propeller would effect on the pressure drop measurement; thus, a dedicated test was performed to investigate the effect of the mixing propeller on the pressure drop measurement. The test was conducted according to the experimental protocol, (see section 5.2), using tap water, with no debris added, and with approaching velocity of 0.519 cm/s. Two measurements were taken; the first one with the propeller OFF for 550 seconds and the second one with the propeller ON for 550 second. The two measurements showed that the effect of the propeller is insignificant as shown in Figure 4.7.

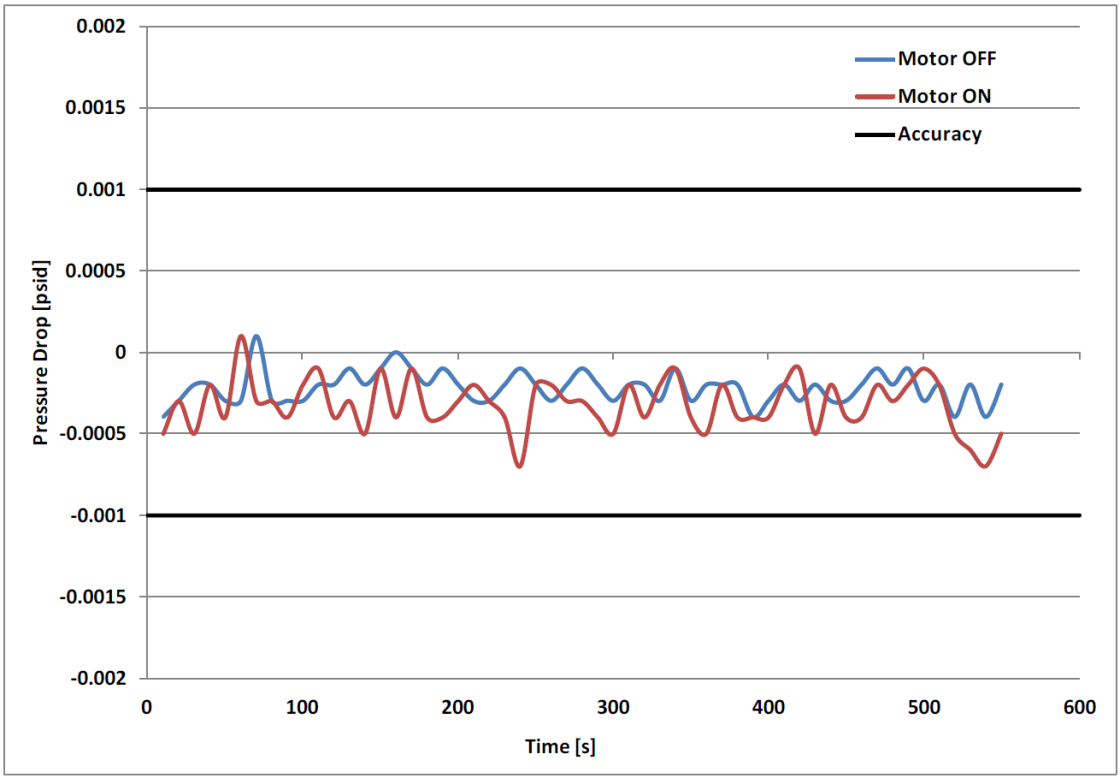

Figure 4.7 Effect of the Mixing Propeller on the Pressure Drop

Figure 4.7 above shows that the effect of the mixing propeller on the pressure drop measurement using a high accuracy differential pressure transducer (see section 4.2.3). It was concluded that the effect of the mixing propeller is insignificant and can be neglected.

4.2.3 Pressure Transducer

A differential pressure transducer (Honeywell TJE) was installed on both sides of the strainer as shown in Figure 4.8. It was concluded from preliminary tests the debris bed can exceed 9 in (22.86cm) in thickness at lower approaching velocity, therefore, the pressure transducer was installed 10 inch (25.4 cm) away from both sides of the strainer. The pressure transducer was connected to the polycarbonate pipes via flexible tubing. The tubing of the pressure transducer were installed on the side of the polycarbonate piping, rather than the top, to eliminate the possibility of trapped micro-bubbles to be transported to the sensors. This unit has a range of 1 pound per square inch differential (psid) and accuracy of 0.001 with a certificate of calibration traceable to the National Institute of Standards and Technology (NIST) [16].

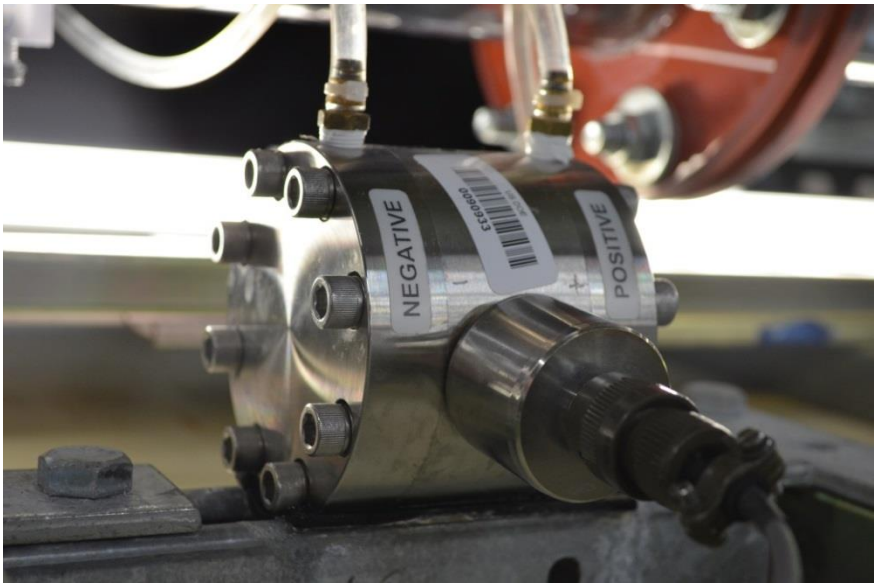

Figure 4.8 Honeywell Pressure Transducer

4.2.4 Ultrasonic Flow Meter

An Optisonic-6400 portable ultrasonic clamp-on flowmeter was installed 80 in (203.2 cm) away from the strainer [17]. This device is designed to measure and log the flow rate of fluids in full pipes without the need for a Data Acquisition (DAQ) system. The accuracy of the device for the designated flow rates of this experimental study ranges between 1.7% and 3% of the measured values. The main reason for using this device was to verify and log the values of the flow rates, rather than controlling them, due to the 30 seconds response time. This device comes in two pieces, the sensors tray and the signal converter as shown in Figure 4.9.

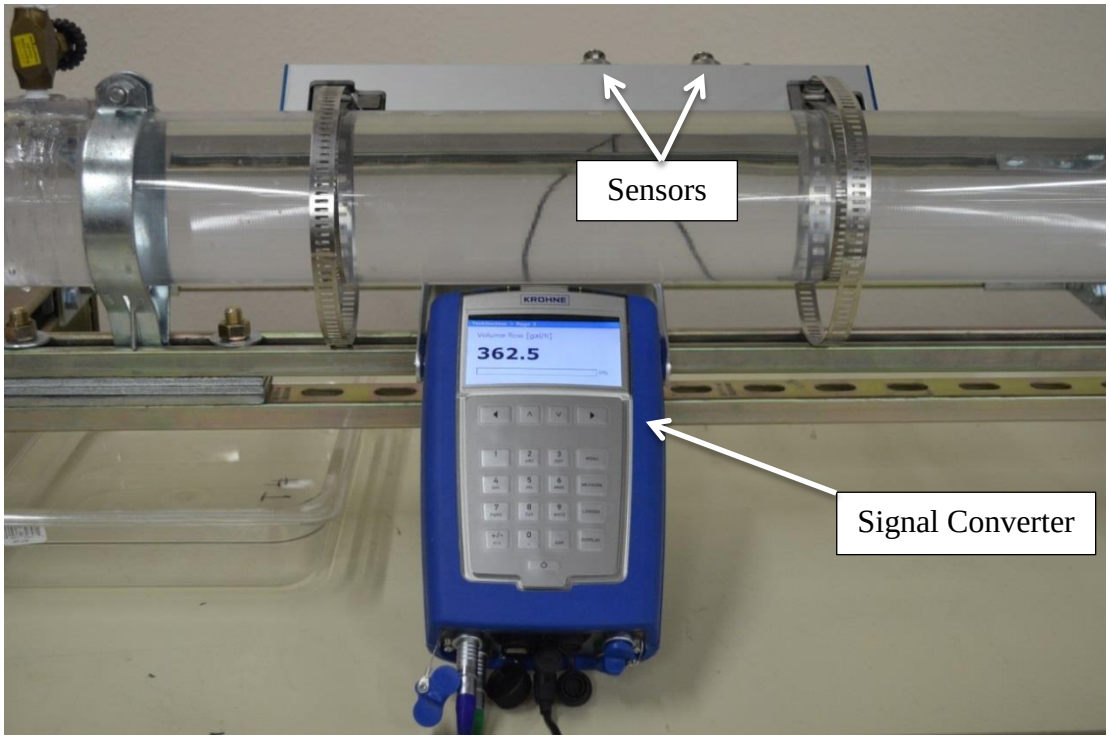

Figure 4.9 Ultrasonic Flowmeter

4.2.4.1 Measuring Principle

This instrument has two transduce that are attached to a line gauged metal tray, this tray fastened directly on the outside of the pipe via mounting straps. The two transducers are connected to a signal converter that display and log the measurements. The measuring principle rely on transmitting and receiving sound waves upstream and downstream the flow as shown in Figure 4.10 Transducer 1 transmit an ultrasonic wave through the pipe wall and into the fluid, the signal travels through the fluid and reflects on the opposite pipe wall and then received by transducer 2, and vice versa [17].

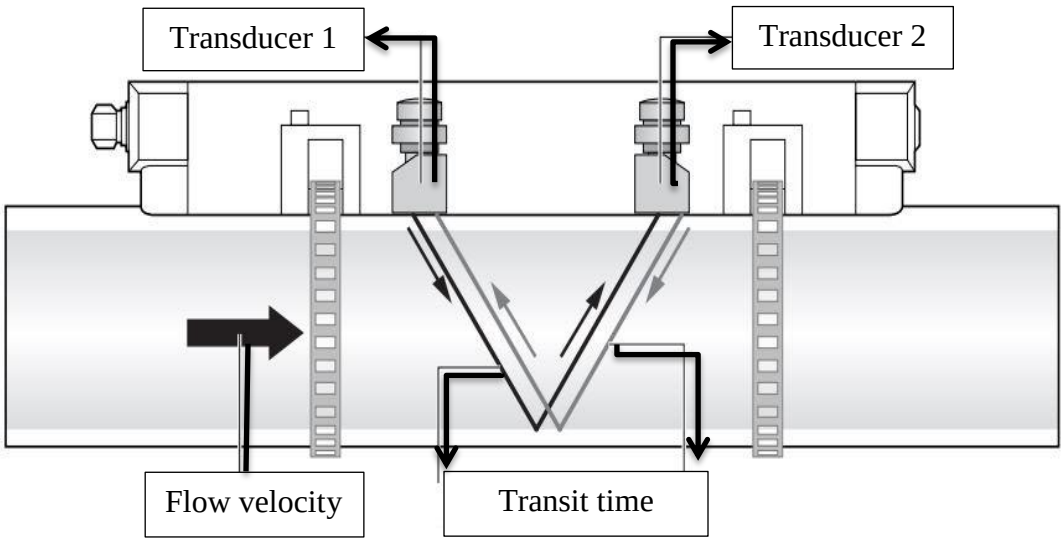

Figure 4.10 Measuring Principle

(Partially taken from Optisonic 6400 Handbook [17])

4.2.5 Flowmeters Assembly

Two flow meters (Rotameters, King®) were installed parallel to each other, sharing the same inlet and outlet, as shown in Figure 4.11.The first flowmeter (7650 Series) was used to control the flow rate for intermediate and maximum range flow rates, it has a range of 300 gallon per hour (GPH) with a full-scale accuracy of ±5%. The second flow meter (K76 Series) was used to control minimum range flow rates, with a range of 60 GPH and a full-scale accuracy of ±3% [18].

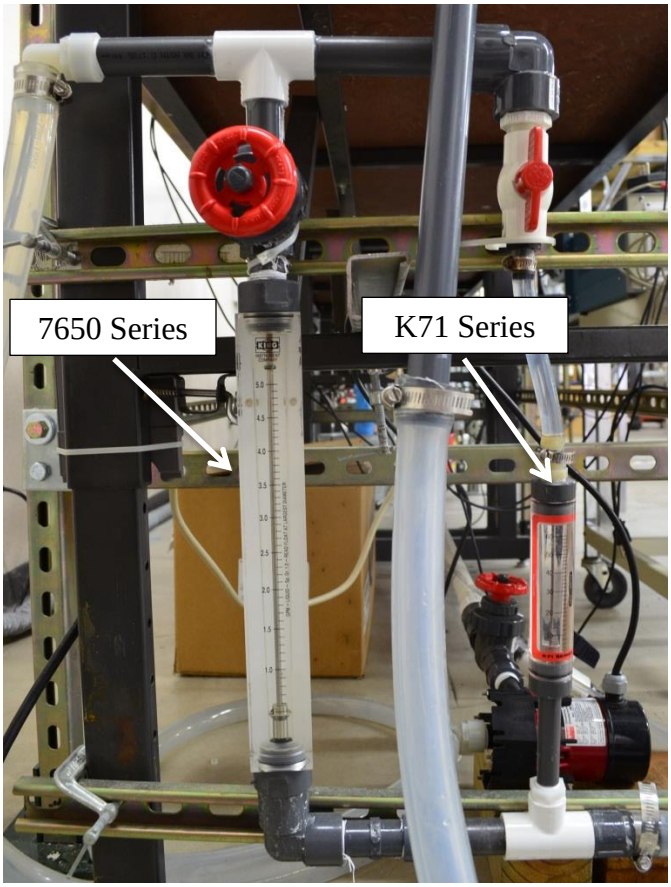

Figure 4.11 Flowmeters Assembly

4.2.6 Circulation Pump

A Dayton® circulation pump (Model 3WY88) was installed to provide the required volumetric flow rate for the flow loop as shown in Figure 4.12. The flowmeters assembly was connected to the pump suction inlet via a 2 in. (5.08 cm) high-pressure flexible tubing to eliminate the effect of the pump vibration on the pressure measurement. The pump outlet was connected to the water tank inlet by a 2 in. (5.08 cm) PVC piping and controlled by a gate valve. The circulation pump can operate under a maximum temperature of 140º F (60 º C) and maximum pressure 50 psi (3.38 bar) with 1/50 horsepower (hp).

Figure 4.12 Circulation pump

4.2.7 Data Acquisition

A Honeywell data acquisition system (Model SC2000) was installed to process and log the data from the differential pressure transducer, as shown in Figure 4.13, with a 10 seconds sampling rate. The DAQ was connected to the pressure transducer via a 12-pin channel connector and to the computer via 25- pin system connector. The choice of the SC200 DAQ was based on its unique features including, but not limited to: automatic setup, calibration, and scaling of strain-gage sensors through the use of Signature Calibration™ [19].

Figure 4.13 SC2000 Data Acuasition Sysytem

4.2.8 High-Definition Camcorder

A Sony digital HD video camera recorder (Model HDR-XR260) [20] was installed, Figure 4.14, on a tripod to record the debris bed build up process during the experiment.

Features:

- 8.9 mega pixels in resolution
- 30x optical zoom
- 55x extended digital zoom
- 160 gigabytes internal hard disc
- 30 Frame per Second (FPS)

Figure 4.14 Sony High-Definition Camcorder

5. TEST PROCEDURE

The experimental facility was prepared and cleaned prior to conducting each experiment, it was insured that the flow system was free of any debris or impurities prior to each experiment. The experimental facility was keenly cleaned before running any test by filling and draining the system simultaneously using tap water for 15 to 20 minutes, this procedure will be referred to as pre-test cleaning. After each experiment, the water in the system was completely discharged and the debris bed accumulated on the system strainer was removed from the strainer surface using a vacuum cleaner. After removing the debris bed, the system was washed and cleaned in order to remove any residual debris from the tank and the strainer. The system was then filled with water and left to run overnight, or at least for 6 hours, this step was performed by temporary installing a filter bag at the tank outlet. Any debris or impurities that might be stuck inside the flow system were collected inside the filter bag. The filter bag was then removed and the cleaning water was drained and prepared for the next test by following the pre-test cleaning procedure. The test procedure is divided into two parts, the first part will be dedicated to explain the debris preparation procedures, and the second part will be dedicated to explain the experimental protocol.

5.1 Debris Preparation Procedure

The NUKON debris preparation process was conducted according to the Nuclear Energy Institute (NEI) protocol report [21]. The material was produced and processed in order to meet the NEI requirement before it is used.

5.1.1 NUKON Debris Sampling and Weighing

It was determined previously that each test in this experimental study should use a quantity of 40 g of NUKON as debris. The desired amount was sampled from a heat treated NUKON matt produced by Performance Contracting Inc. (PCI), the NUKON mats produced by the manufacturer has dimension of 2.5" x 24" x 48". It was observed that the sides of the NUKON mat were overheated during the production process, thus, the sides of the mat may have different material properties than the middle of the mat. To avoid any undesired uncertainties that might come from using the overheated sides and to insure that all tests have the same characteristics of the NUKON mat, all samples were taken from the middle of the NUKON mat as shown in Figure 5.1. The sample taken from the matt have, on average, dimensions of 2.5" x 4.5" x 5.5" each sample was weighted on an ACCUALAB® scale (Model # V-2400) with range of 2400 g and full scale accuracy of 0.1g as shown in Figure 5.2. Each sample was trimmed from the side repeatedly until the desired weight of 40 g was achieved.

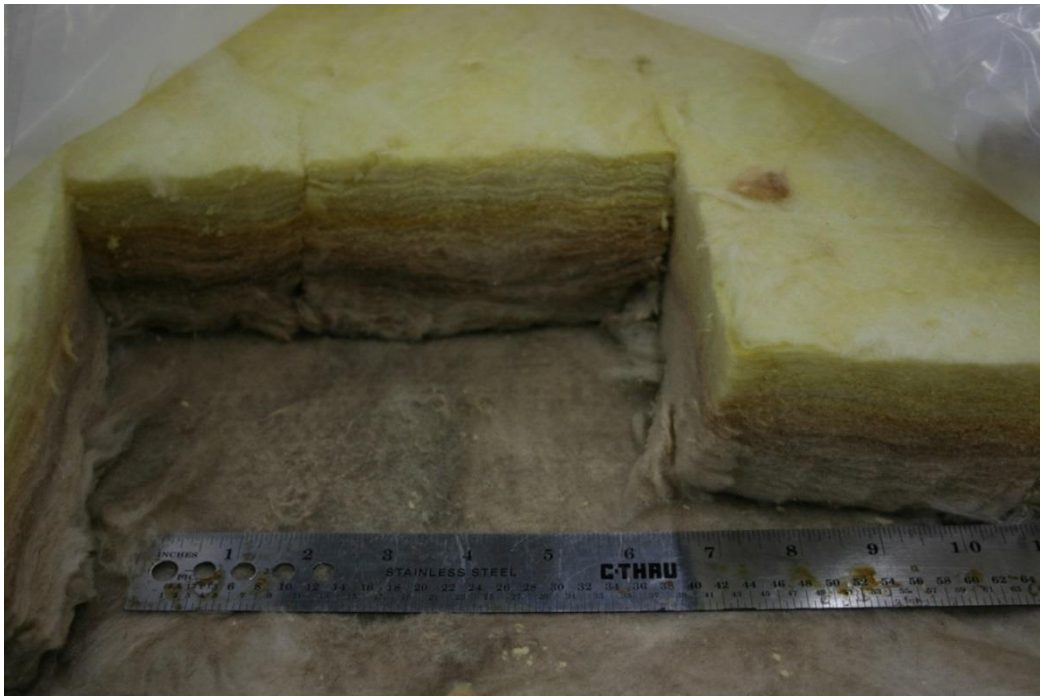

Figurer 5.1 NUKON Mat

Figure 5.2 NUKON Sampling and Weighting

5.1.2 Debris Size Reduction

In this step, the NUKON sample of 40 g was separated horizontally into four layers, the original sample was first separated into two layers, a dark layer and a light layer, each layer was then separated into two more layers. The four layers were approximately of the same thickness, the two dark layers are corresponding to the side of the mat that was in contact with the heating surface during the production process, and the two light layers are corresponding to the opposite side of the matt away from the heating surface. The layer separation process was conducted inside the preparation bucket to preserve the original mass of the sample and to prevent any loss of smaller bits as shown in Figure 5.3. Each layer was then cut into smaller pieces of approximately the same size, it was insured during the cut process that none of the smaller pieces should exceeded 1" x 1" x 1". The pieces from the light layers were additionally torn in half, since the stiffer than the pieces from the dark layers. All the smaller pieces were then put in a plastic bucket, also called the preparation bucket, as shown in Figure 5.4. The preparation bucket has a total capacity of 5 gallons (18.93 liter), it was washed and cleaned before and after each preparing process, small amount of water was added in the bucket, about 0.5 gallon, just about enough to slightly cover the smaller pieces. The bucket was covered with the preparation lid to prevent the pieces from flying off the bucket during the next step.

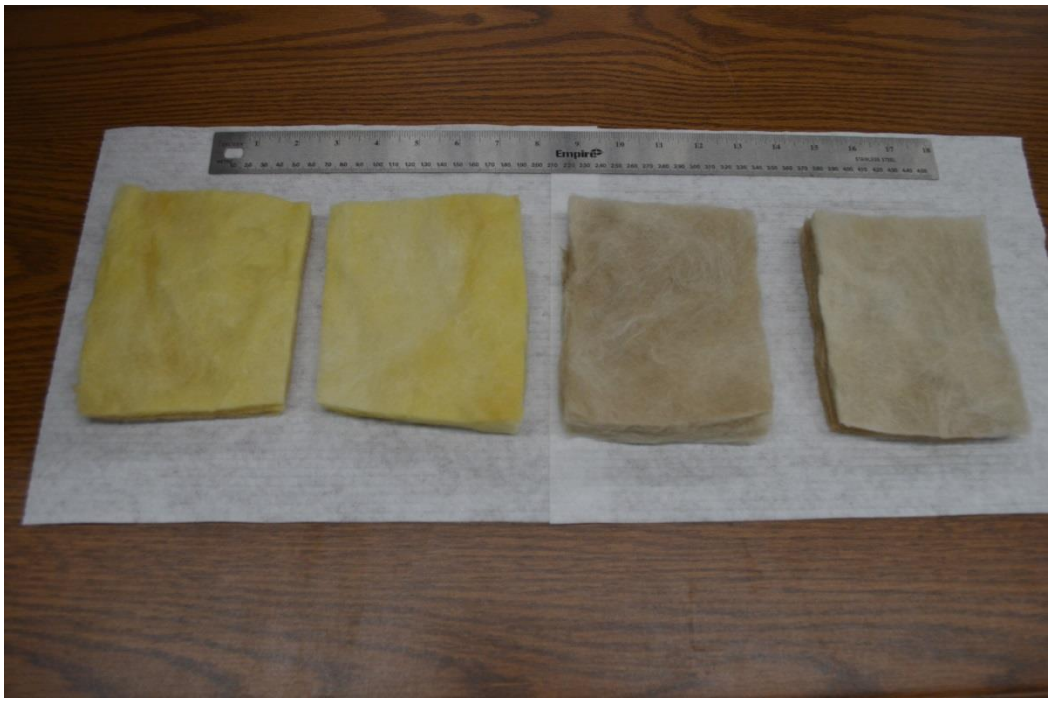

Figure 5.3 Layer Separation

Figure 5.4 Preparation Bucket

5.1.3 High Pressure Water Jet

A high pressure washer with 1800 psi jet pressure and 1.5 GPM (5.68 l/m) flow rate, as shown in Figure 5.5, was used to breakdown and mix the debris inside the preparation bucket via jet nozzle with angle of 40º [22]. The jet gun was inserted into the bucket through the preparation lid as sown in Figure 5.6. The water jet was kept submerged slightly below the water level in the bucket during the operation and the jet gun was moved randomly inside the bucket to allow uniform breaking and mixing. The washer jet was turned off when the water level inside the bucket reached the 4 gallon marker, this amount of water jet was sufficient to allow a uniform breaking and mixing as shown in Figure 5.7.

Figure 5.5 CLEANFORCE® High Pressure Washer

Figure 5.6 Debris Breaking and Mixing

Figure 5.7 Final State of the Debris Sample

5.2 Experimental Protocol

After cleaning the system facility as explained earlier in this section and preparing the debris sample following the debris NEI preparation procedure, explained in section 5.1, each test was conducted in the order of the steps listed below.

- The designated strainer was installed (STP versus Vogtle)
- The flow system was filled with tap water until that water level in the tank reached 18.75 inch.
- All the bubbles trapped on the upper side of the pipe wall were removed using the venting valve shown in Figure 5.8.

Figure 5.8 Venting Valve

- The mixing propeller was switched on and the time delay relay was set to alternate the direction of rotation every 5 minutes
- All bubbles were released from the pressure transducer tubing before resetting the device
- The system flow rate was adjusted to the designated approaching velocity
- The system was left to run for approximately 10 minutes to maintain steady flow rate
- The pressure transducer was reset through the DAQ
- The DAQ software was prepared to log the pressure date ,with 10 seconds sampling rate, in an excel spreadsheet file
- The Camcorder was set on a tripod approximately 50 cm away from the strainer
- The prepared debris sample was re-mixed inside the preparation bucket
- The DAQ logger and the Camcorder were both triggered at the same time
- The debris sample was poured inside the water tank within a 5 second period
- The water level inside the tank reached 20 in. after adding the debris sample
- The temperature of the system was verified to be 24±3º C
- The test was left to run for 18 hours or until reaching study state whichever occurs first
- Pictures of the final debris bed thickness were taking before the test was terminated
- The system was cleaned and prepared for the next test as explained before.

6. RESULTS AND DISCUSSION

The results were compared based on the designated approaching velocities and the strainer type. Three tests were run for each case using STP strainer and two tests were run for each case for the Vogtle strainer, 15 tests in total, as shown in Tables 6.1 and 6.2. The reason behind repeating the tests was to study the uncertainty and the repeatability of the results.

Table 6.1 STP Strainer Experimental Results

STP Strainer			
Approaching Velocity	0.311 cm/s	1.167 cm/s	3.112 cm/s
Steady state Pressure Drop (psid)	0.0293	0.1583	0.6256
	0.0288	0.1665	0.6406
	0.0331	0.1705	0.6362

Table 6.2 Vogtle Strainer Experimental Results

Vogtle Strainer			
Approaching Velocity	0.311 cm/s	1.167 cm/s	3.112 cm/s
Steady state Pressure Drop (psid)	0.0245	0.1658	0.5471
	0.0236	0.1295	0.5439

6.1 STP Strainer Results

Nine tests were performed using the STP strainer and the results were compared to each other based on the approaching velocity range. Three tests for each approaching velocity were performed and the results were compared to each other based on the pressure drop and the debris bed thickness.

6.1.1 Minimum Approaching Velocity (0.311 cm/s)

For this approaching velocity, it took about 127 minutes for the water in the tank to overturn one time, completely through the whole system, (one turnover). The system reached an average steady state pressure drop of 0.030 psid after approximately 11 hours (660 minutes) as shown in Figure 6.1. It took the system about 5 turnovers for all the debris to be filtered out from the tank via the strainer and the debris bed accumulated on the system strainer. Each test was conducted for about 20 hours with an average thickness of 10.51 inch (26.71 cm) as shown if Figure 6.2. The average debris bed thickness was measured for each experiment individually using the *10 points method*: a method used in previous work. In this method, the buildup of the debris bed on the strainer can be studied by drawing 10 points with uniform spacing along the axial direction of the bed as shown in Figure 6.3. This image processing method was used to plot the debris bed build up against time as shown in Figure 6.4. The average bed thickness was also plotted as a function of time (Figure 6.5) and pressure (Figure 6.6).

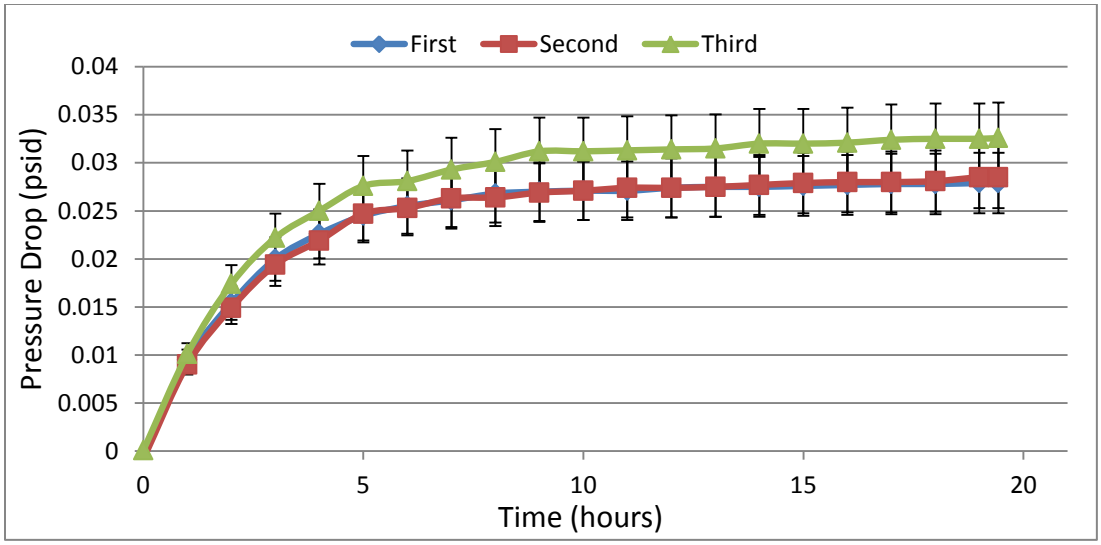

Figure 6.1 Head Loss Data (STP Strainer, STDEV ±11.3%, 0.311 cm/s, 40g)

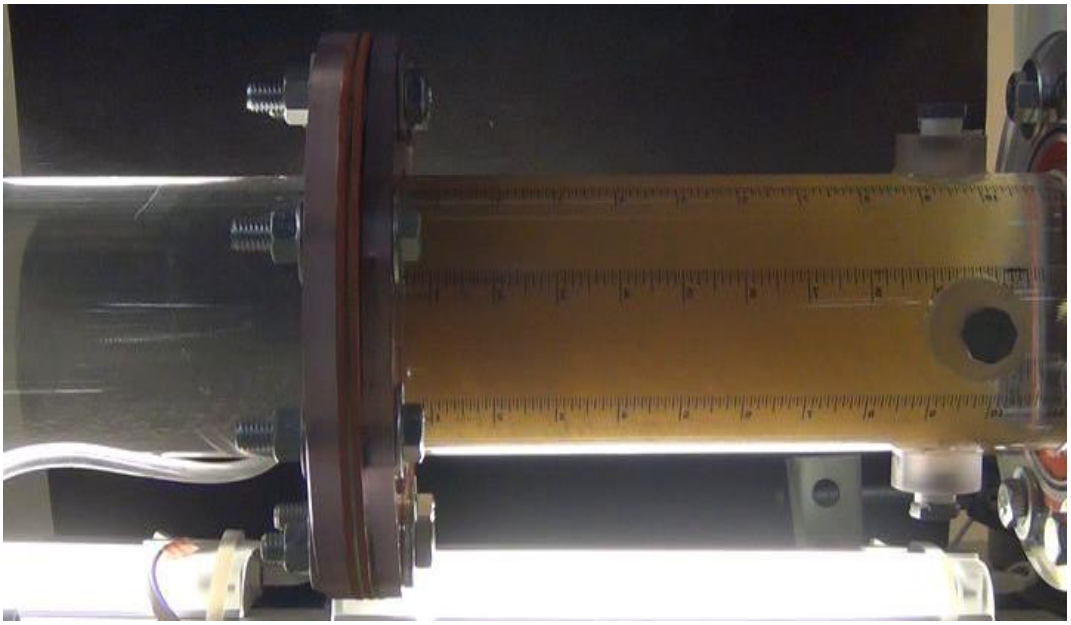

Figure 6.2 Final Debris Bed Thickness (STP Strainer, 0.311 cm/s, 40g)

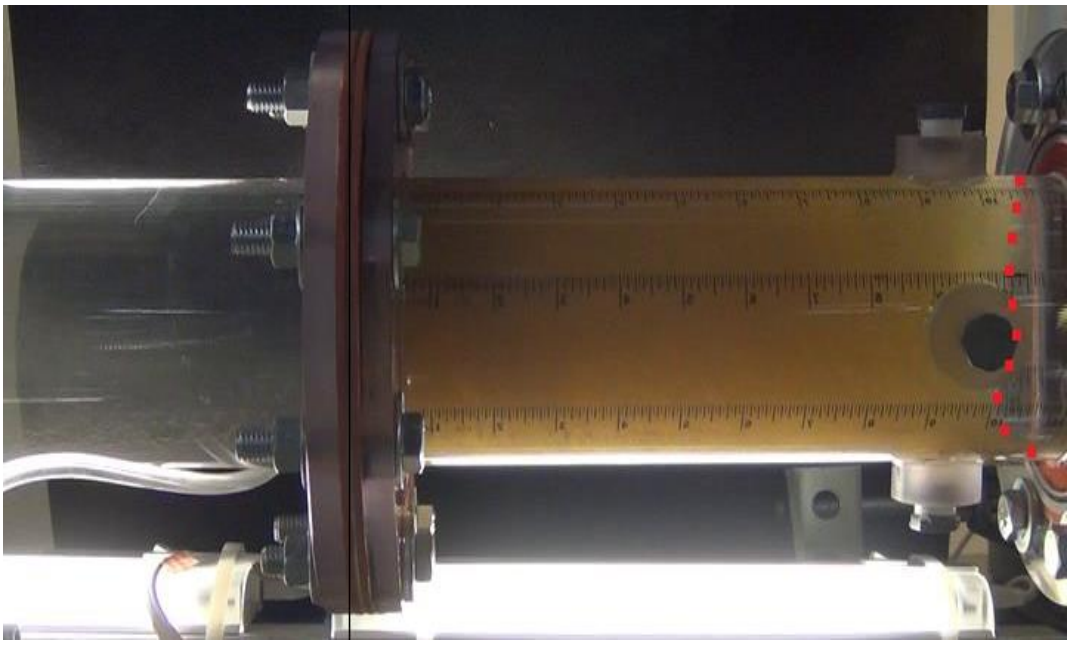

Figure 6.3 The 10 Points Method

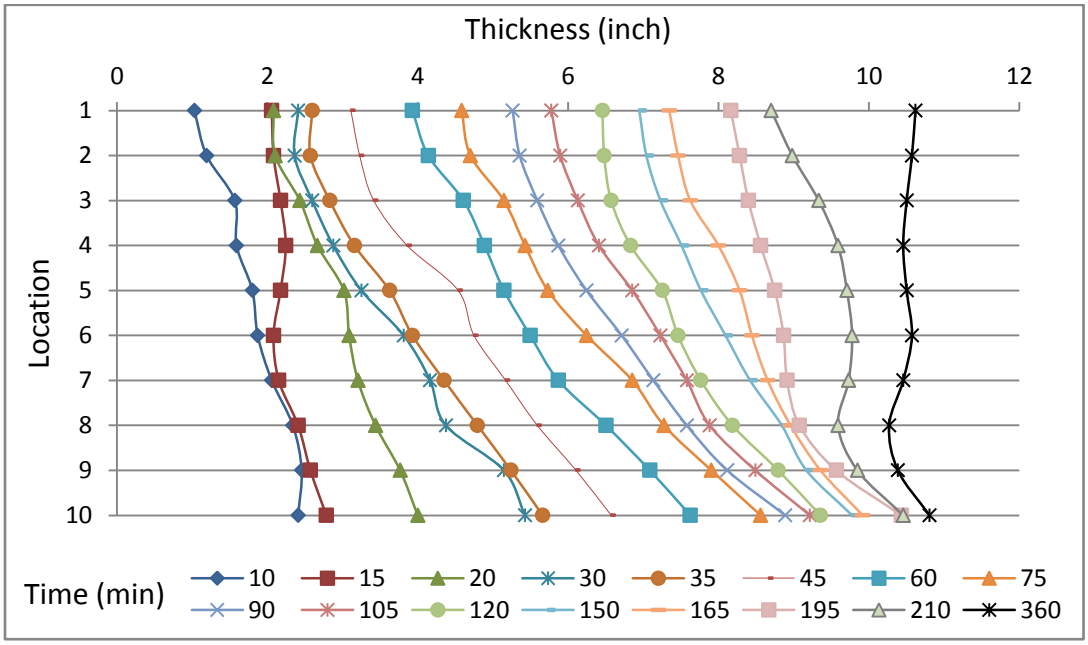

Figure 6.4 Debris Bed Buildup over Time (STP Strainer, 0.311 cm/s, 40g)

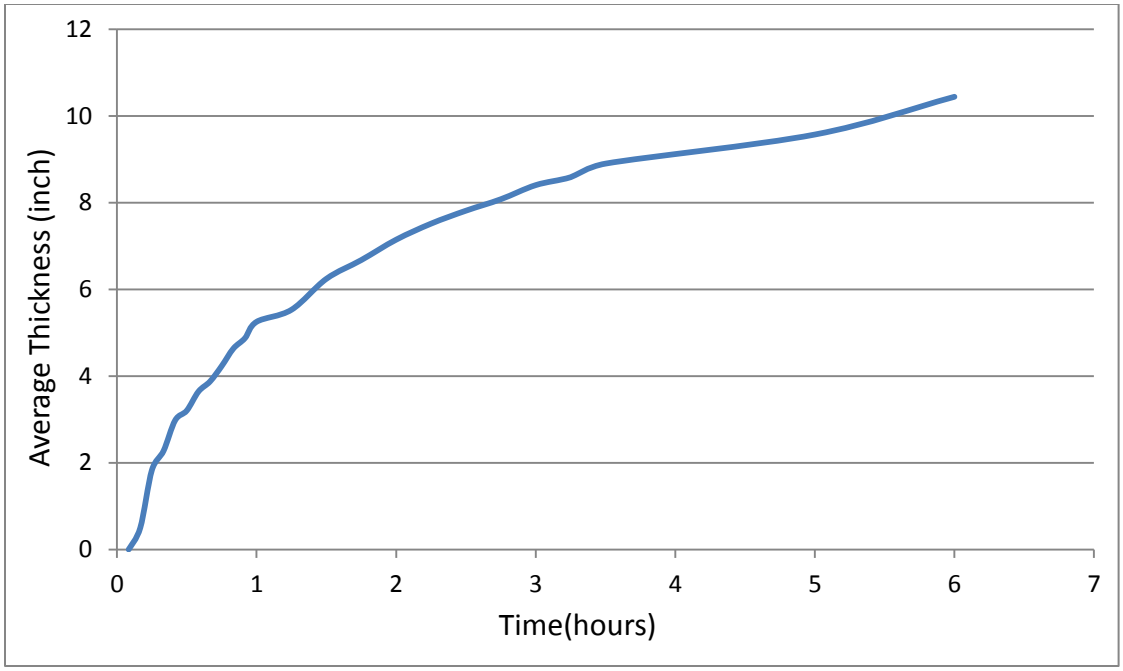

Figure 6.5 Debris Bed Thickness over Time (STP Strainer, 0.311 cm/s)

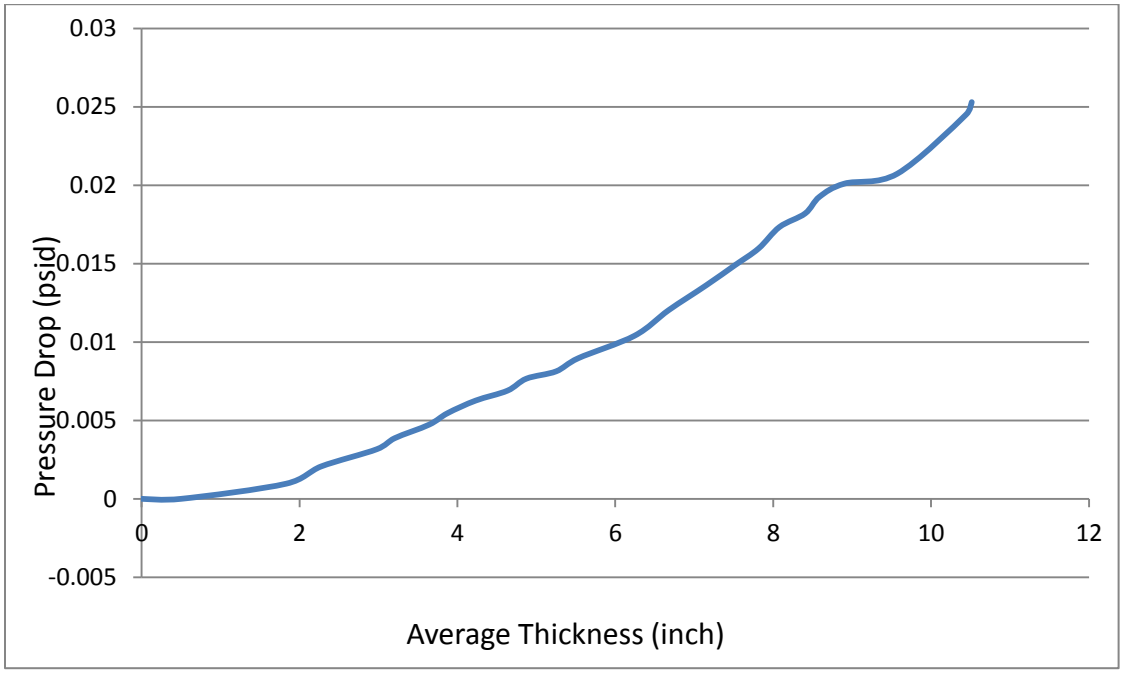

Figure 6.6 Pressure Drop as a Function of Thickness (STP Strainer, 0.311 cm/s)

6.1.2 Intermediate Approaching Velocity (1.167 cm/s)

For this approaching velocity, it took about 34 minutes for the water in the tank to undergo one turnover. The system reached an average pressure drop of 0.165 psid after 3 hours (180 minutes) as shown in Figure 6.7. It took the system about 5 turnovers for all the debris to be filtered out from the tank via the strainer and the debris bed accumulated on the system strainer. The system was left to run for about 17 hours in order to study the effect of the system flow on the final bed thickness. The final debris bed has an average thickness of 6.13 inch (15.57 cm) as shown in Figure 6.8. The debris bed build up was plotted as a function of time (Figure 6.9), the average bed thickness was also plotted as a function of time, as shown in Figure 6.10, and pressure, as shown in Figure 6.11.

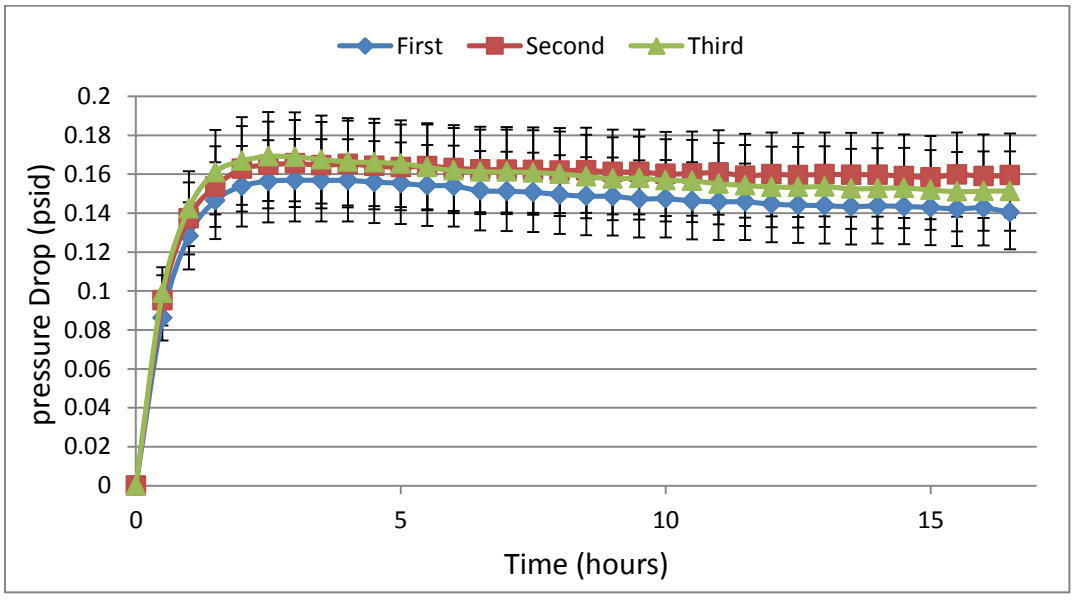

Figure 6.7 Head Loss Data (STP Strainer, STDEV ±13.5%, 1.167 cm/s, 40g)

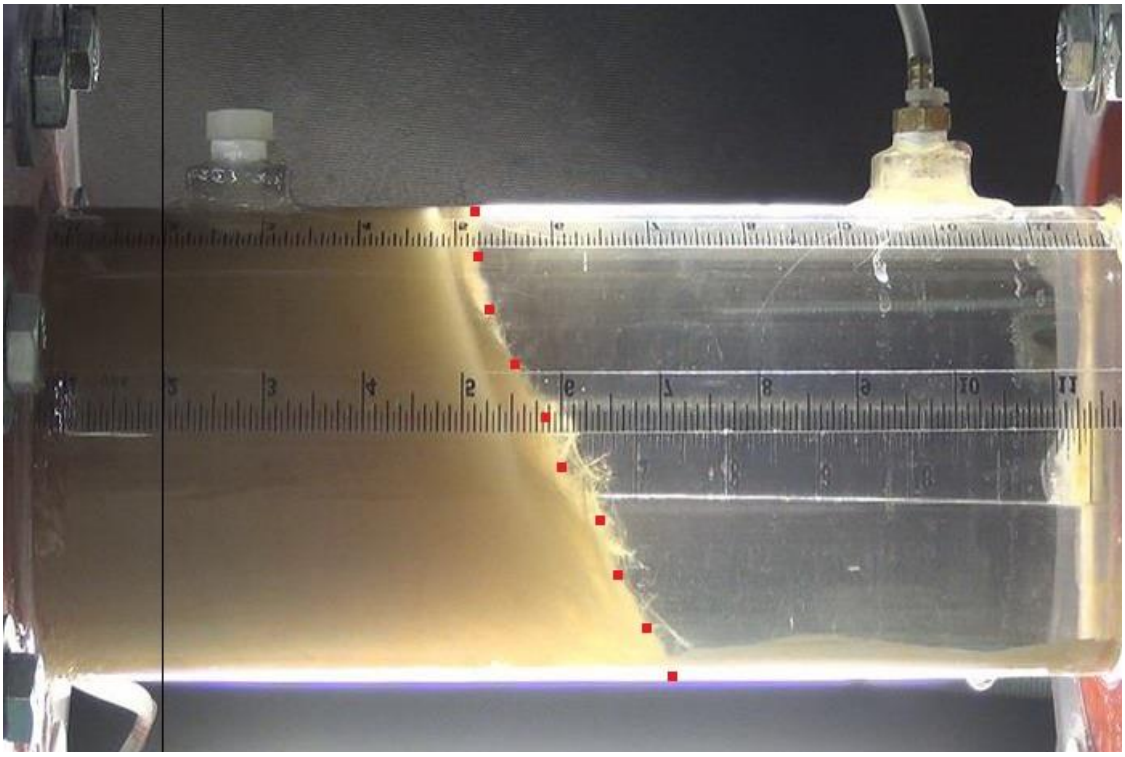

Figure 6.8 Final Debris Bed Thickness (STP Strainer, 1.167 cm/s, 40g)

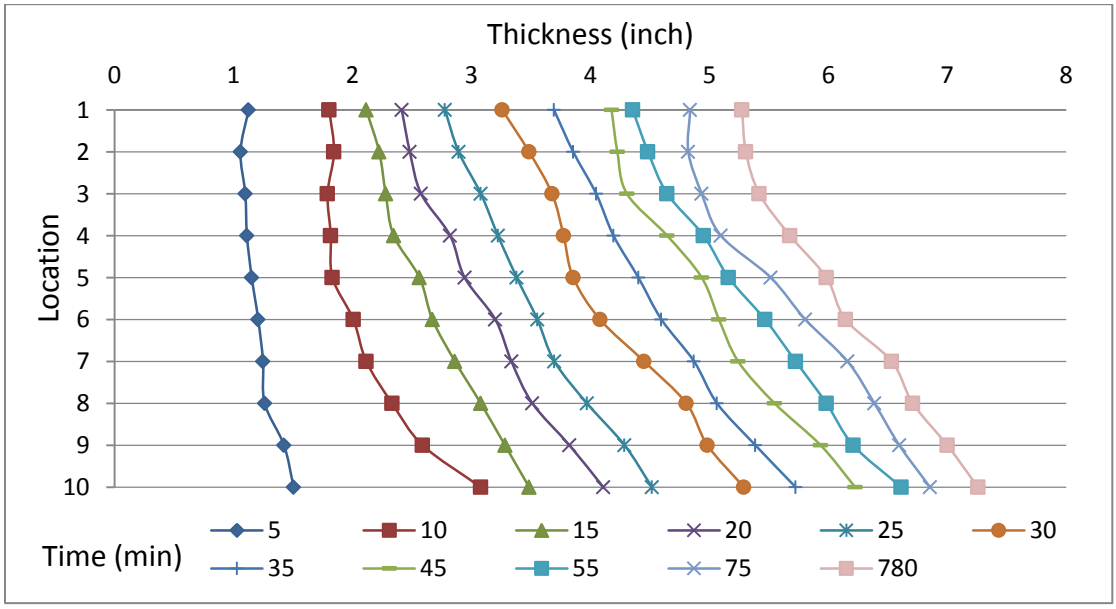

Figure 6.9 Debris Bed Buildup over Time (STP Strainer, 1.167 cm/s, 40g)

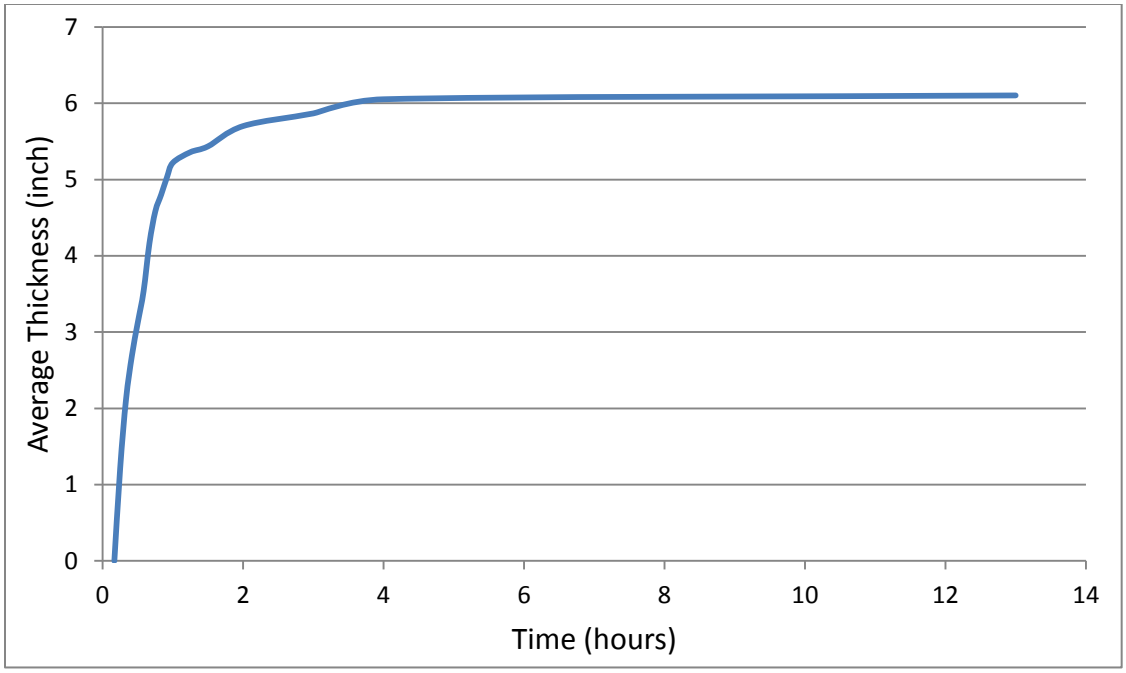

Figure 6.10 Debris Bed Thickness over Time (STP Strainer, 1.167 cm/s, 40g)

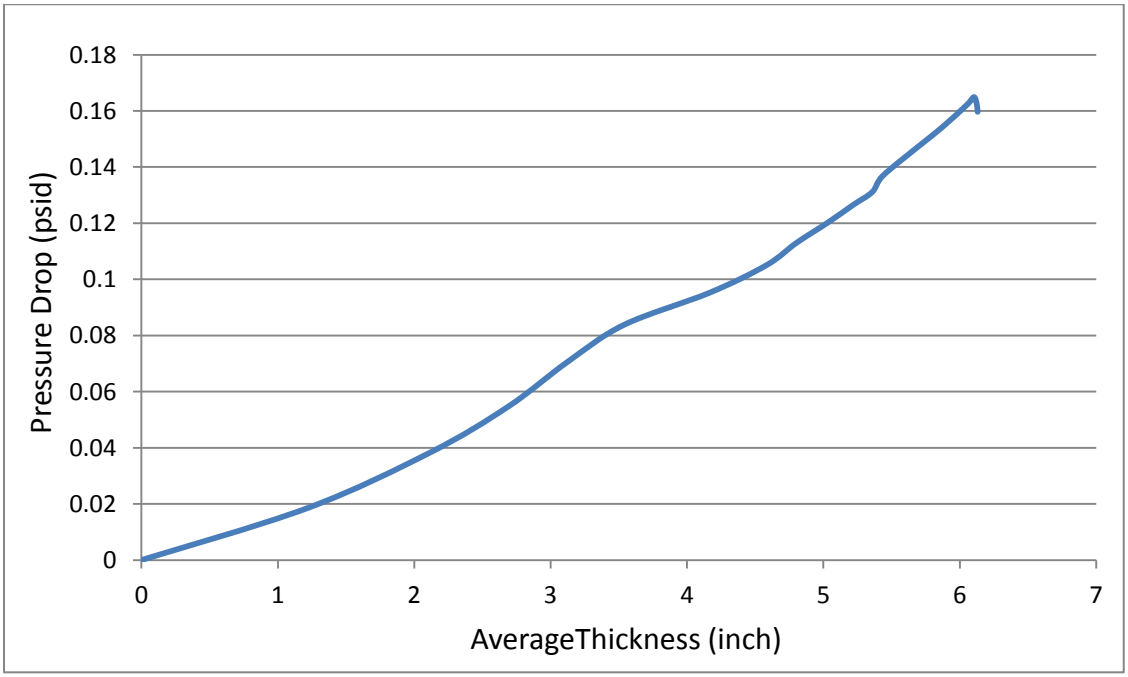

Figure 6.11 Pressure Drop as a Function of Thickness (STP Strainer, 1.167 cm/s)

6.1.3 Maximum Approaching Velocity (3.112 cm/s)

For this approaching velocity, it took about 13 minutes for the water in the tank to undergo one Turnover. The system reached steady state pressure drop of 0.634 psid after about 1 hour (60 minutes) as shown in Figure 6.12. It took the system about 5 turnovers for all the debris to be filtered out from the tank via the strainer and the debris bed accumulated on the system strainer. Even though the test reached steady state after about 1 hour, the system was left to run for about15 more hours in order to study the effect of the system flow on the final bed thickness. The final debris bed has an average thickness of 4.53 inch (11.52 cm) as shown in Figure 6.13. The bed build up was plotted for given time intervals (Figure 6.14), The average bed thickness was also plotted as a function of time, as shown in Figure 6.15., and pressure, as shown in Figure 6.16.

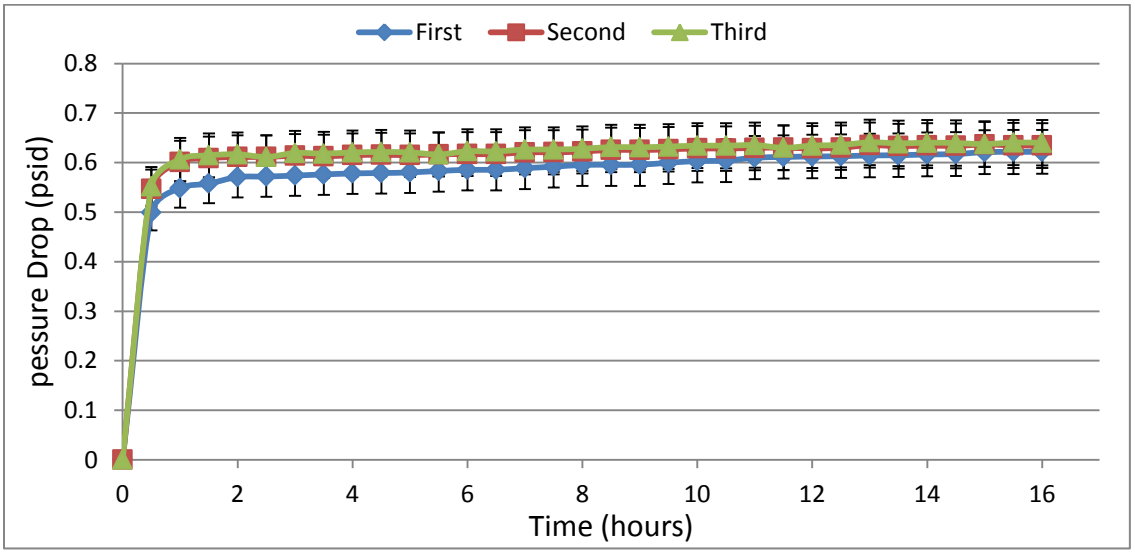

Figure 6.12 Head Loss Data (STP Strainer, STDEV ±7.15%, 3.112 cm/s, 40g)

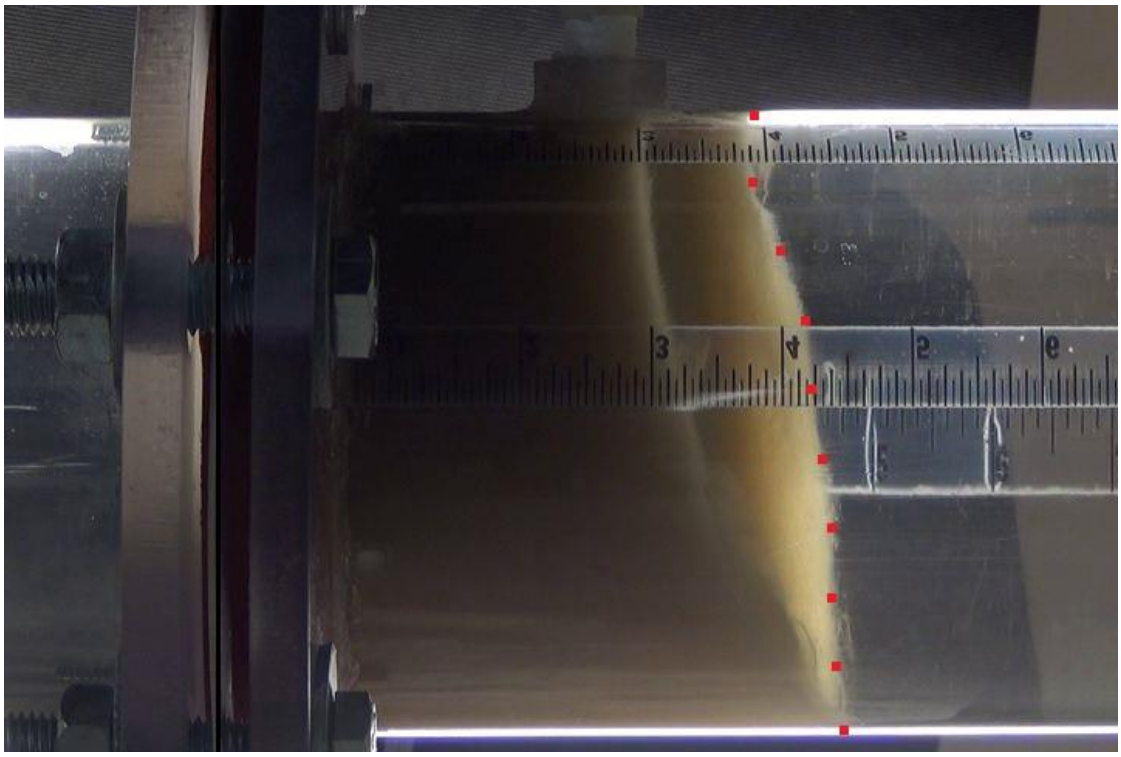

Figure 6.13 Final Debris Bed Thickness (STP Strainer, 3.112 cm/s, 40g)

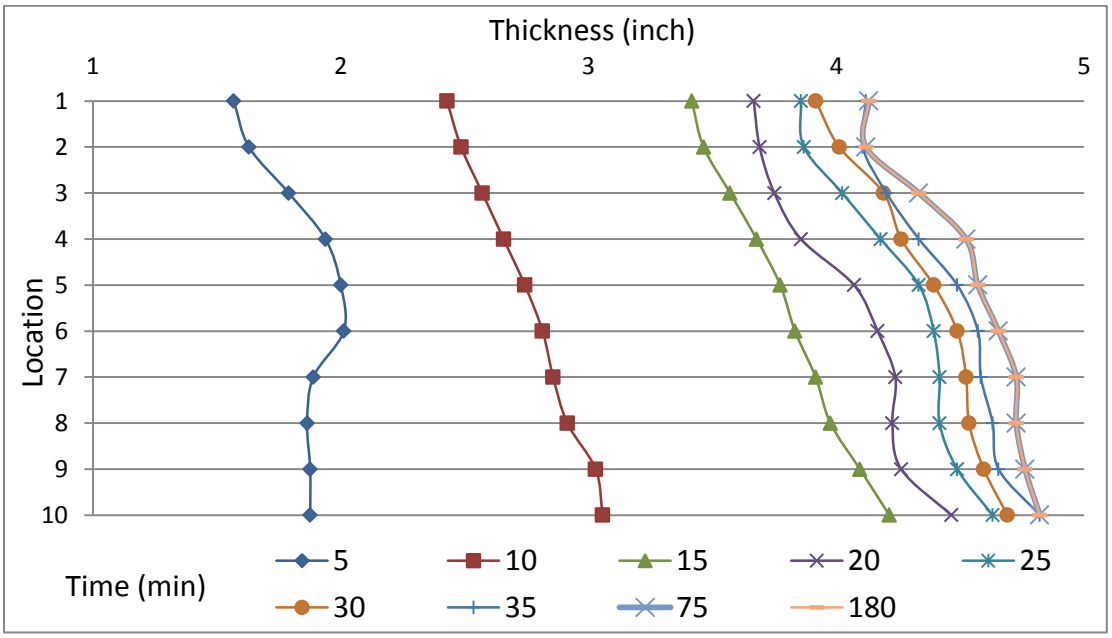

Figure 6.14 Debris Bed Buildup over Time (STP Strainer, 3.112 cm/s, 40g)

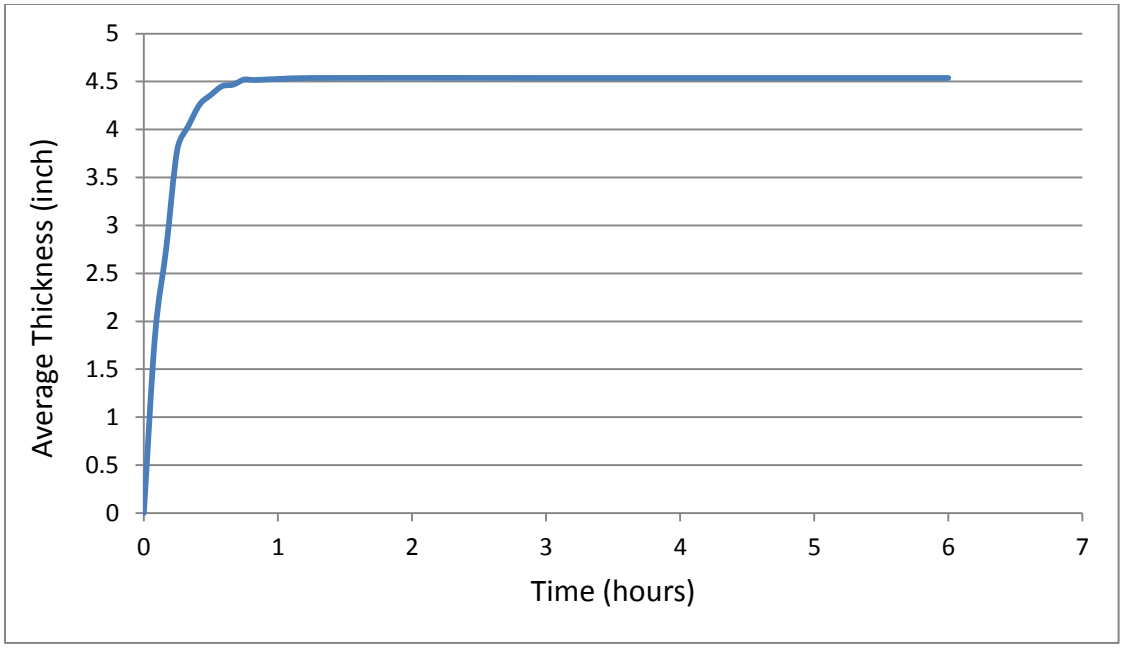

Figure 6.15 Debris Bed Thickness over Time (STP Strainer, 3.112 cm/s, 40g)

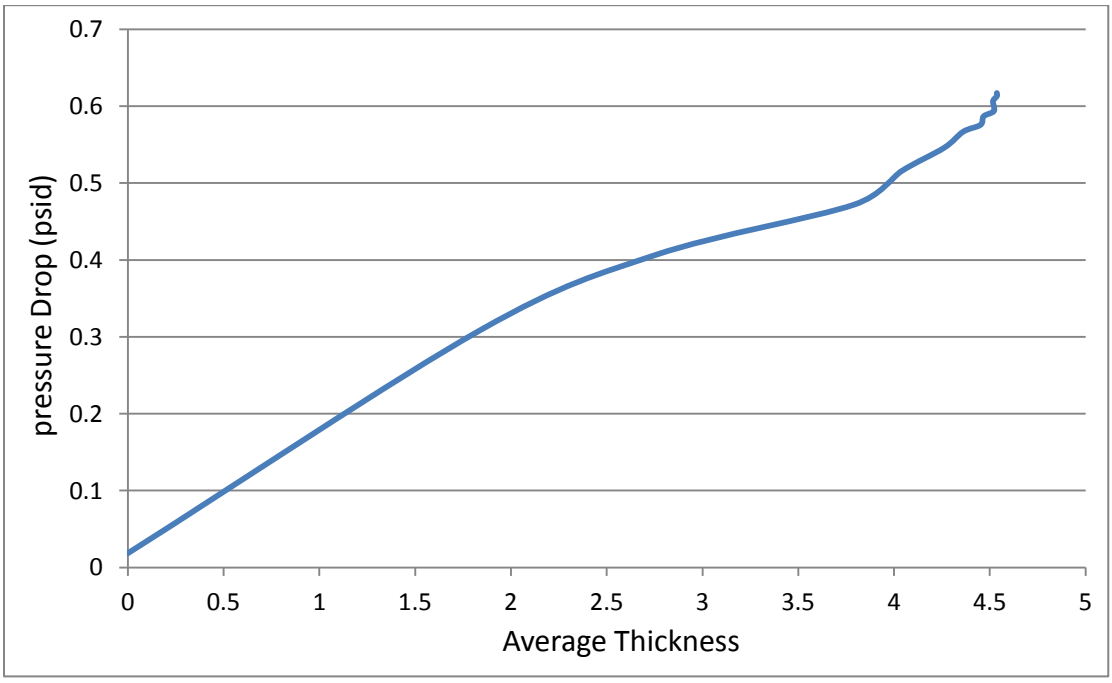

Figure 6.16 Pressure Drop as a Function of Thickness (STP Strainer, 3.112 cm/s)

6.1.4 Comparison and Discussion

One test for each approaching velocity was analyzed by calculating the average bed thickness at designated time intervals using the 10 pints method. For each selected time interval, the pressure drop corresponding to that time interval was calculated by averaging the pressure drop values for 10 second before and 10 seconds after the designated time. The calculated pressure drop was plotted against time for each approaching velocity as shown in Figure 6.17.

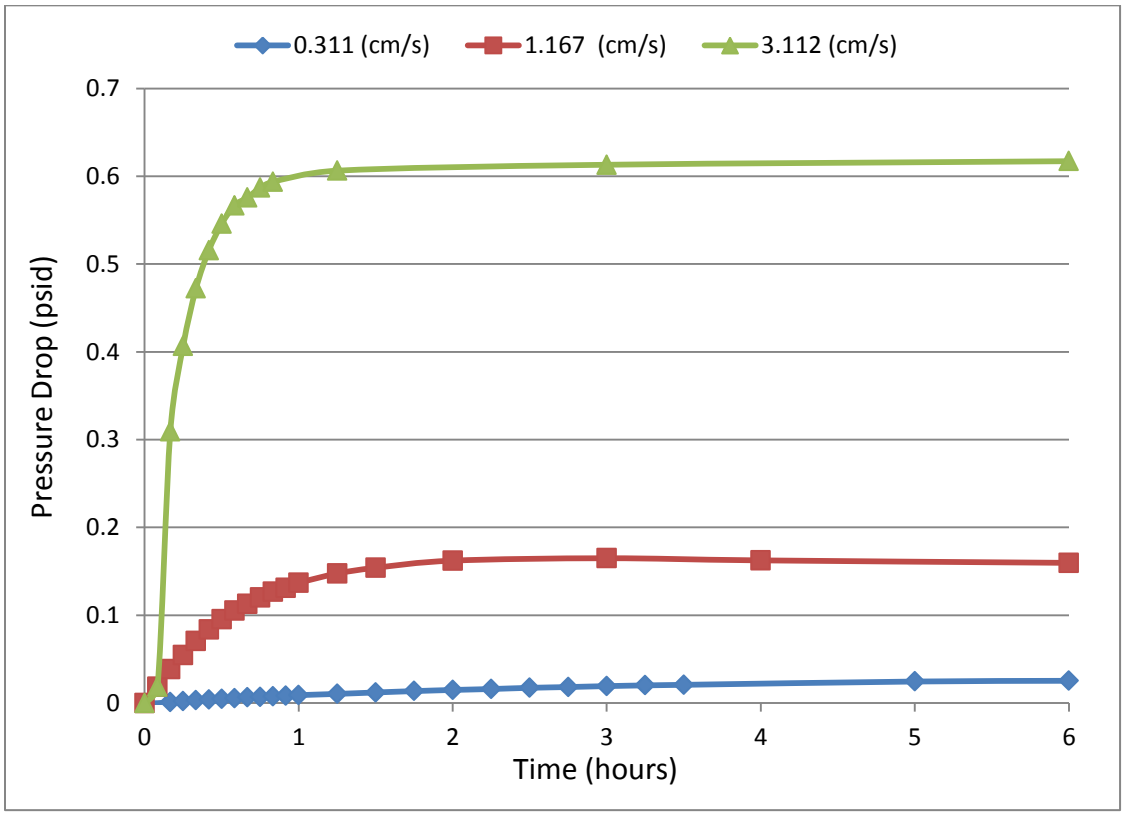

Figure 6.17 Pressure Drop at Different Approaching Velocities (STP Results)

The steady sate pressure drop for the minimum approaching velocity (0.311 cm/s) was about 0.030 psid on average, and the pressure drop for the Intermediate range (1.167 cm/s) was about 0.165 psid on average, which is more than five times higher than the head loss for the minimum range. The pressure drop for the maximum range (3.112 cm/s) was about 0.634 psid, which is almost four times higher than the intermediate range and a more than 20 times the minimum range. The final average bed thickness for the minimum approaching velocity was larger than 10.52 inch, it should be noted that for the minimum range approaching velocity, the final average bed thickness was calculated at 6 hours rather than the end of the experiment time (20 hours), due to the experiment limitations The final debris bed for the intermediate range was about 6.13 inch, which is about 40% less than the minimum range. The final average debris bed for the maximum range was about 4.54 inch, which is about 25% less than the intermediate range and 57% less than the minimum range. The average bed thickness for each test was plotted against time and compared to each other as shown in Figure 6.18. The pressure drop was plotted as a function of the average bed thickness to study the effect of the flow rate on the debris bed thickness. It was observed that higher flow rates affected the shape of the debris bed and increased the head loss due to the compression of the debris bed that caused by the liquid inertia, which in turn, effect other parameter such as volume, density and porosity. For higher approaching velocities, the pressure drop and the debris bed thickness have a non-linear relationship as shown in Figure 6.19.

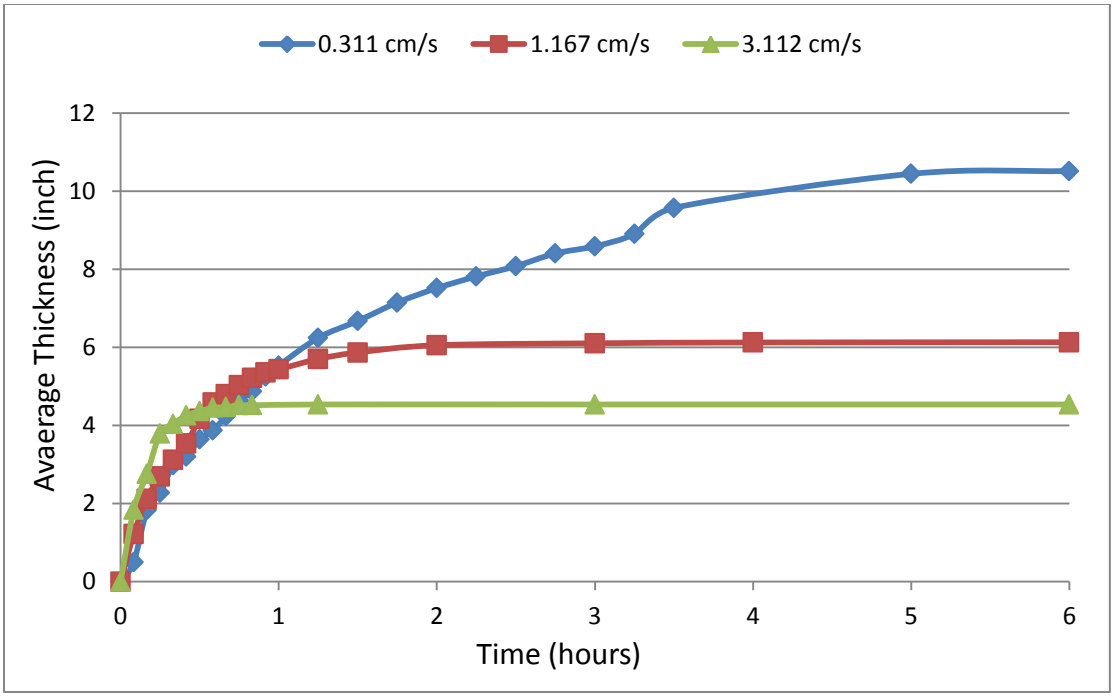

Figure 6.18 Average Debris Bed Thickness over Time (STP Results)

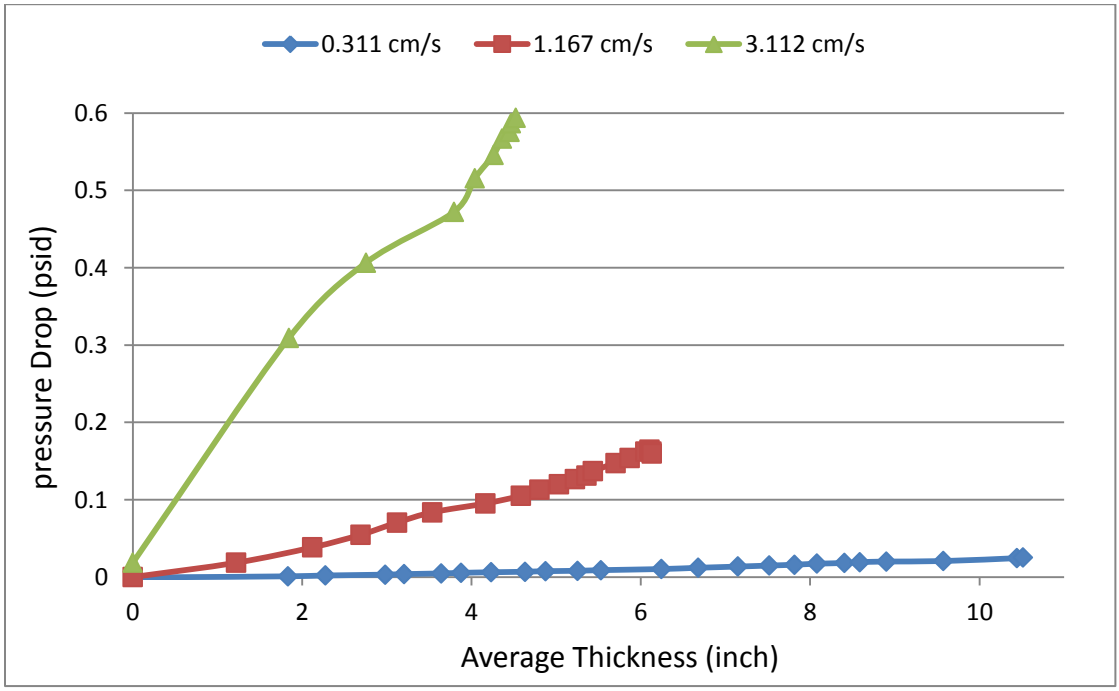

Figure 6.19 Pressure Drop as a Function of Thickness (STP Results)

6.2 Vogtle Strainer Results

Six tests were performed using the Vogtle strainer and the results were compared to each other based on the approaching velocity range. Two tests for each approaching velocity were performed and the results were compared to each other based on the pressure drop and the debris bed thickness.

6.2.1 Minimum Approaching Velocity (0.311 cm/s)

Two tests were performed for this approaching velocity; it took about 127 minutes for the water in the tank to undergo one turnover. The system reached an average steady state pressure drop of psid after about11 hours (660 minutes) as shown in Figure 6.20. It took the system about 5 turnovers for all the debris to be filtered out from the tank via the strainer and the debris bed accumulated on the system strainer. Even though the test reached steady state after about 11 hours, the system was left to run for about 5 more hours in order to study the effect of the system flow on the final bed thickness. The final debris bed has an average thickness of 11.34 inch (28.81 cm) as shown if Figure 6.21. The buildup of the debris bed on the strainer using the 10 points method is shown in Figure 6.22.The average bed thickness was also plotted as a function of time, as shown in Figure 6.23, and pressure, as shown in Figure 6.24.

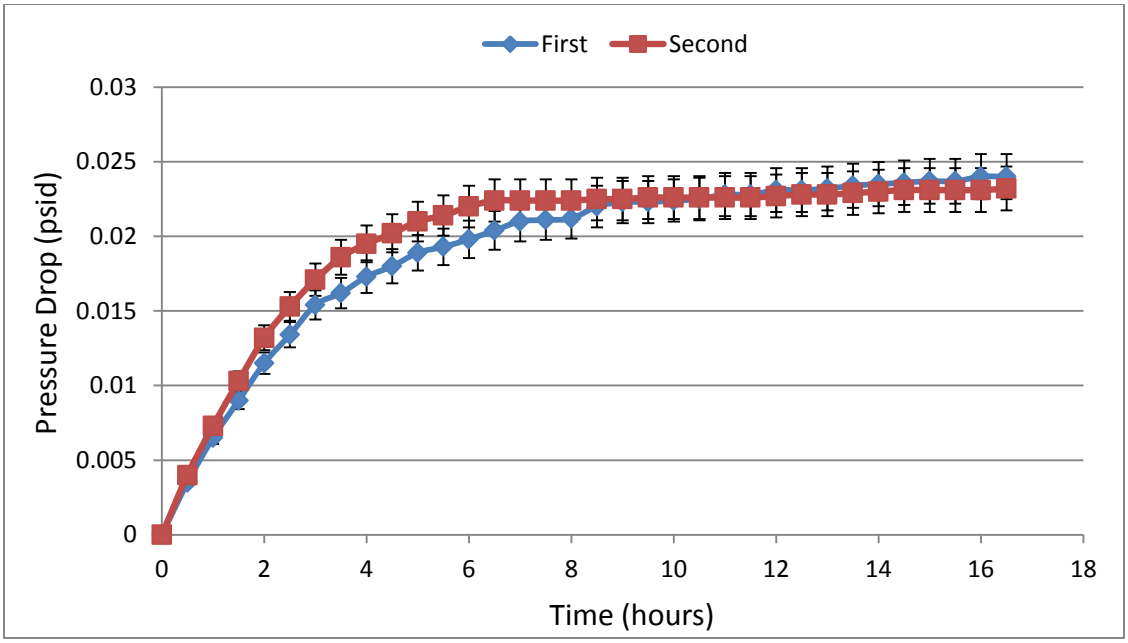

Figure 6.20 Head Loss Data (Vogtle Strainer, STDEV ±6.33%, 0.311 cm/s, 40g)

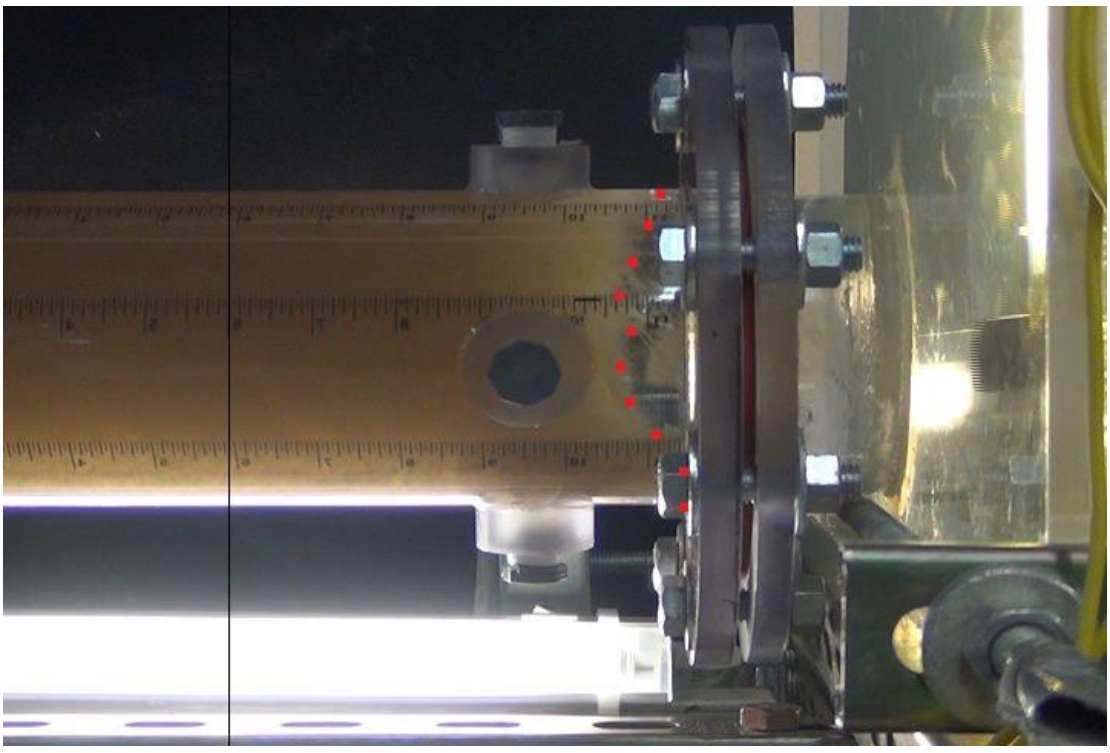

Figure 6.21 Final Debris Bed Thickness (Vogtle Strainer, 0.311 cm/s, 40g)

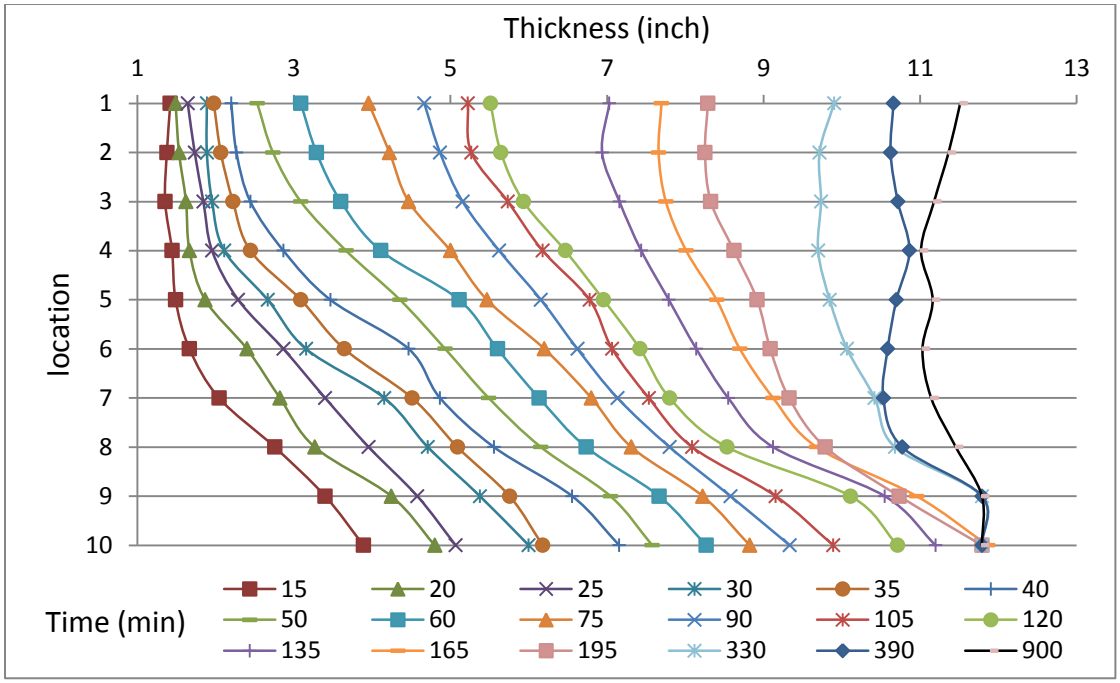

Figure 6.22 Debris Bed Buildup over Time (Vogtle Strainer, 0.311 cm/s, 40g)

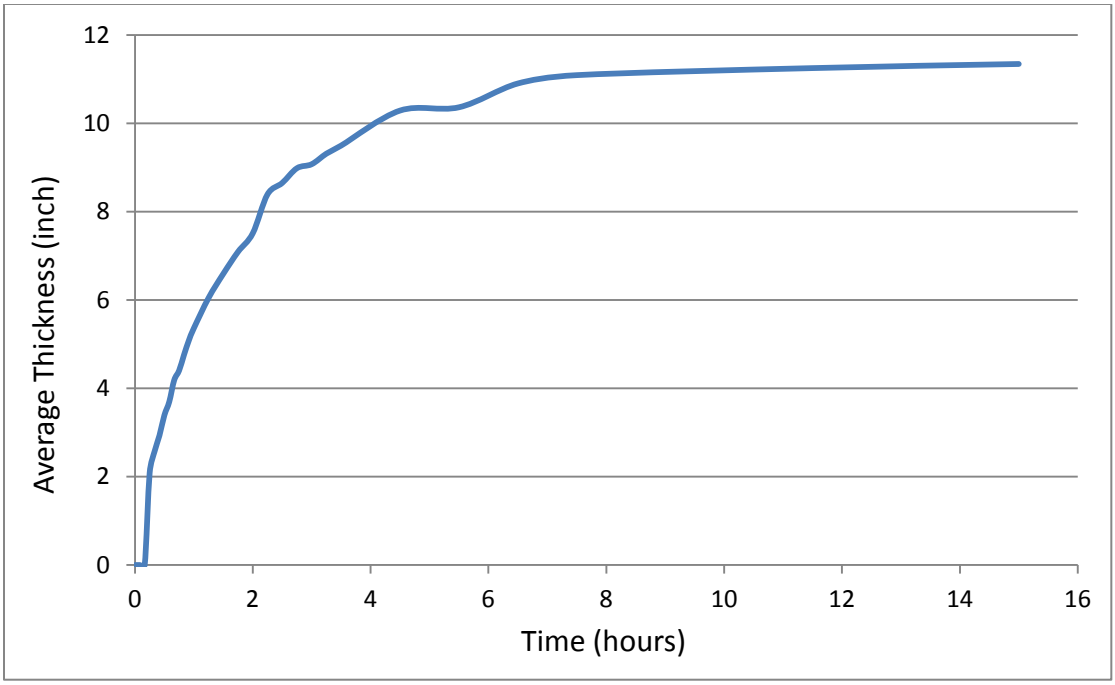

Figure 6.23 Pressure Drop as a Function of Thickness (Vogtle, 0.311 cm/s, 40g)

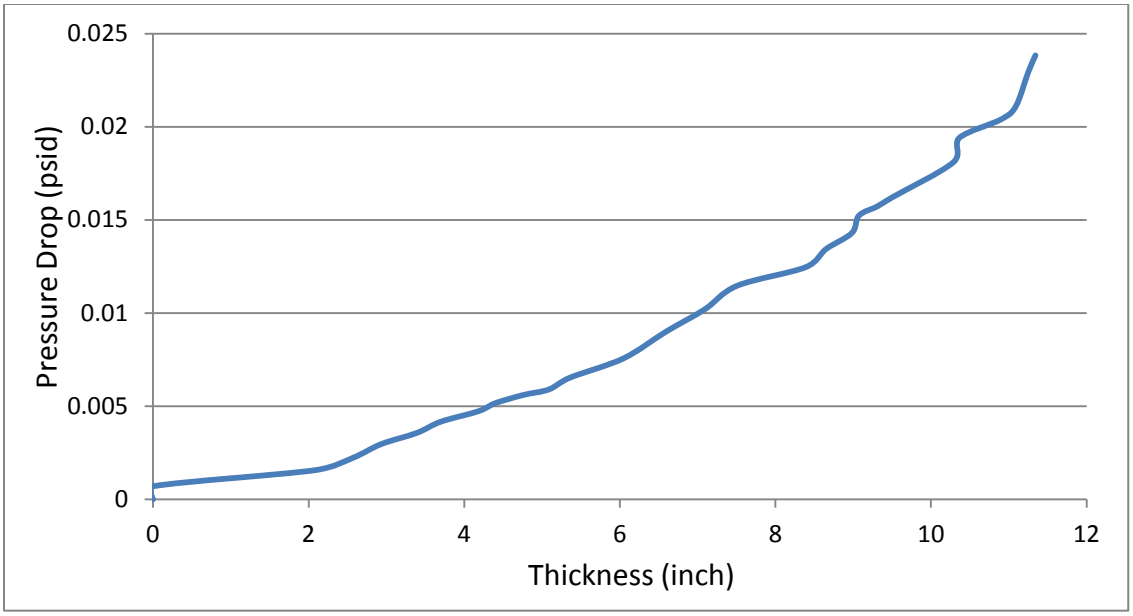

Figure 6.24 Pressure Drop as a Function of Thickness (Vogtle, 0.311 cm/s)

6.2.2 Intermediate Approaching Velocity (1.167 cm/s)

For this approaching velocity, it took about 34 minutes for the water in the tank to undergo one turnover. The system reached maximum pressure drop of 0.1377 psid after 3 hours (180 minutes) as shown in Figure 6.25. The system was left to run for about 17 hours in order to study the effect of the system flow on the final bed thickness. The final debris bed has an average thickness of 7.54 inch (19.15 cm) as shown in Figure 6.26. The buildup of the debris bed on the strainer using the 10 points method is shown in Figure 6.27. The average bed thickness was also plotted as a function of time, as shown in Figure 6.28, and pressure, as shown in Figure 6.29.

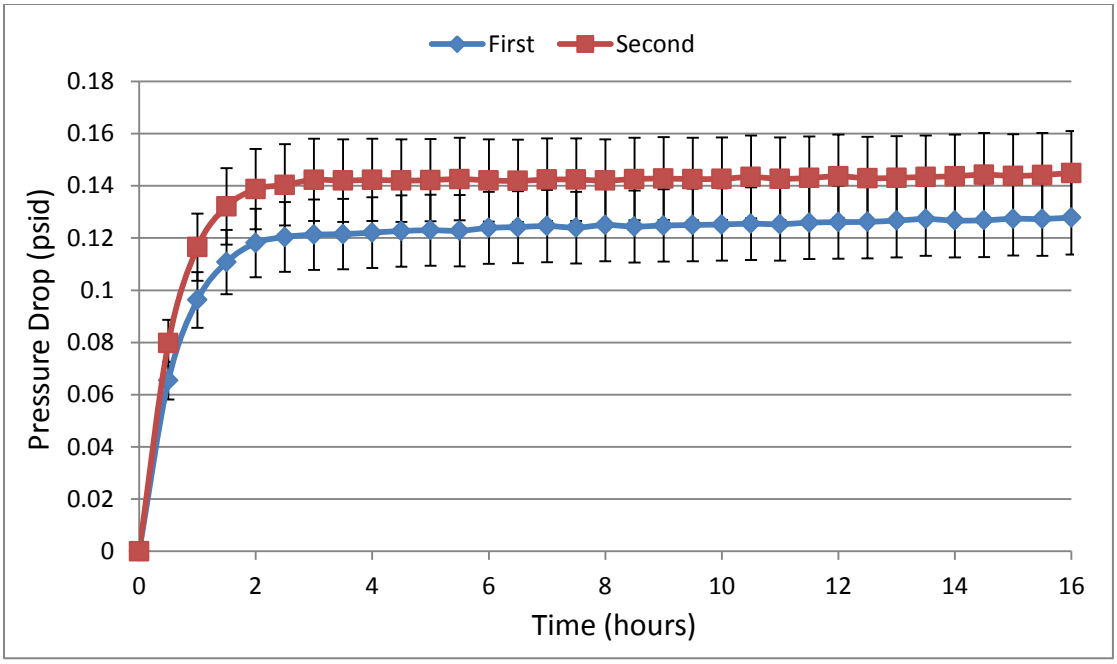

Figure 6.25 Head Loss Data (Vogtle Strainer, STDEV ±11.1%, 0.311 cm/s, 40g)

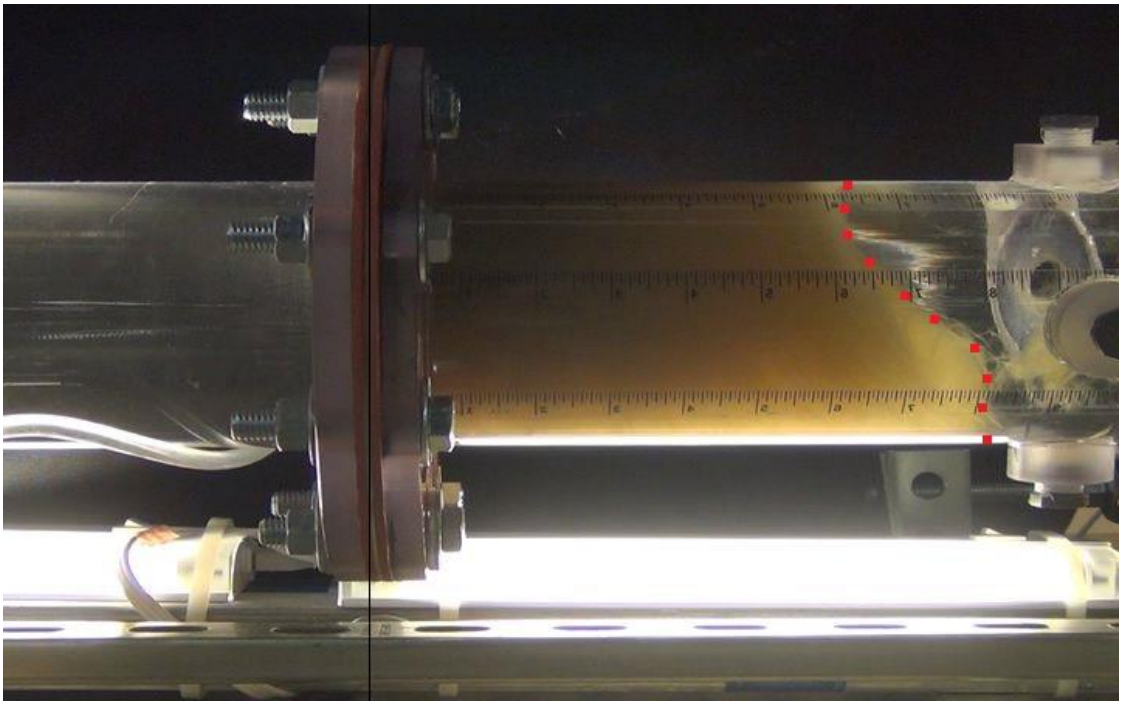

Figure 6.26 Final Debris Bed Thickness (Vogtle Strainer, 1.167 cm/s, 40g)

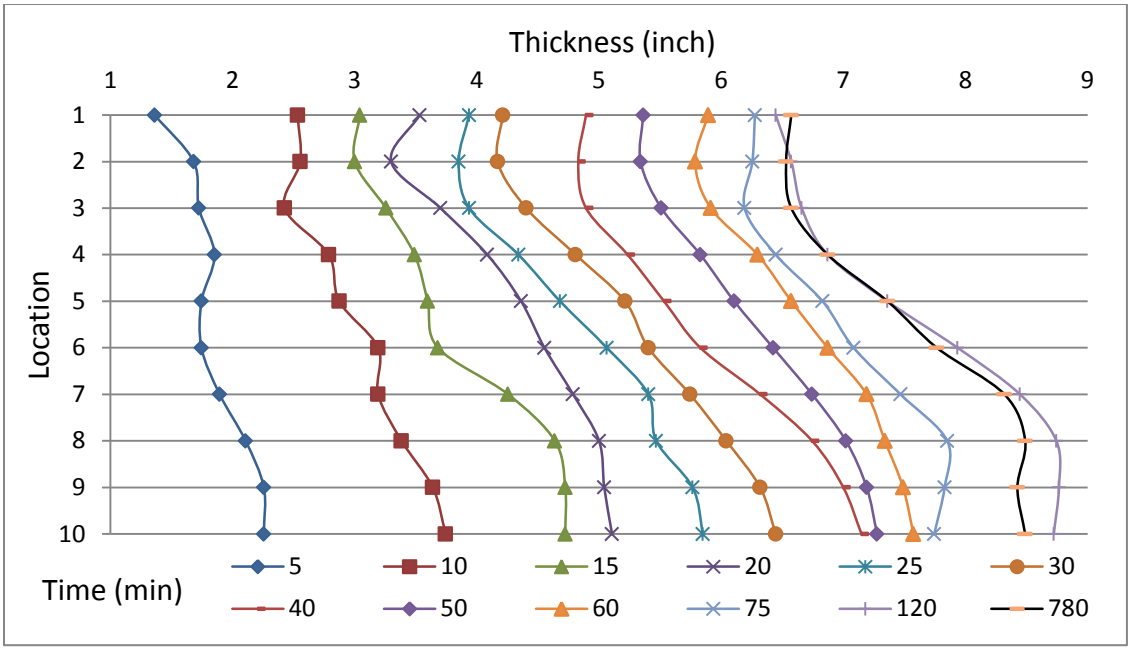

Figure 6.27 Debris Bed Buildup over Time (Vogtle Strainer, 1.167 cm/s, 40g)

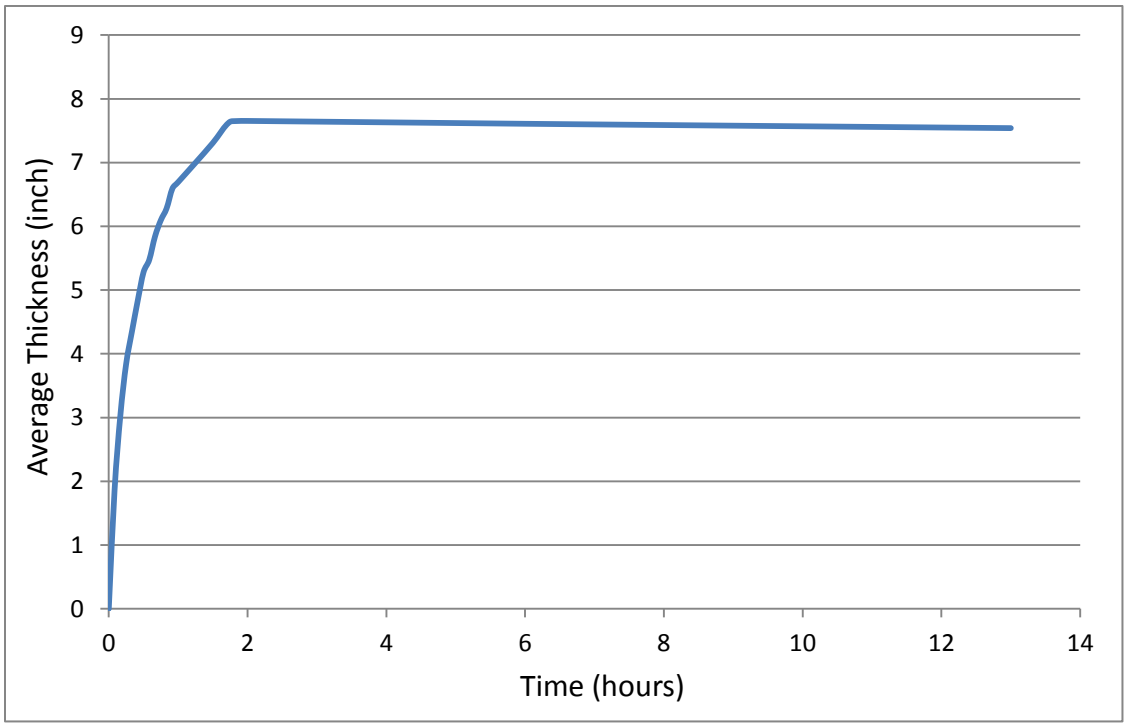

Figure 6.28 Debris bed Thickness over Time (Vogtle Strainer, 1.167 cm/s, 40g)

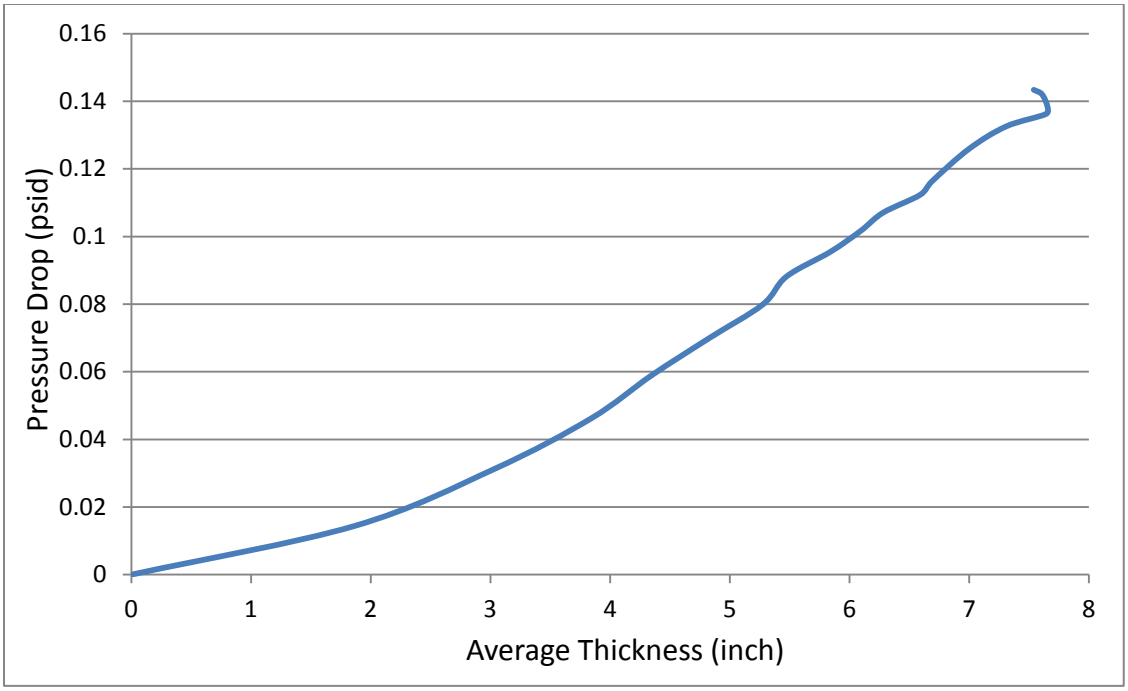

Figure 6.29 Pressure Drop as a Function of Thickness (Vogtle, 1.167 cm/s)

6.2.3 Maximum Approaching Velocity (3.112 cm/s)

Two tests were performed for this approaching velocity; it took about 13 minutes for the water in the tank to undergo one Turnover. The system reached steady state pressure drop of 0.5439 psid after about 1 hour (60 minutes) as shown in Figure 6.30. The test was run for about15 hours in order to study the effect of the system flow on the final bed thickness. The final debris bed has an average thickness of 4.52 inch (11.49 cm) as shown in Figure 6.31. The bed thickness buildup was plotted using the 10 points method as shown in Figure 6.32. The bed thickness and pressure were plotted as a function of time as shown in Figure 6.33 Figure 6.34.

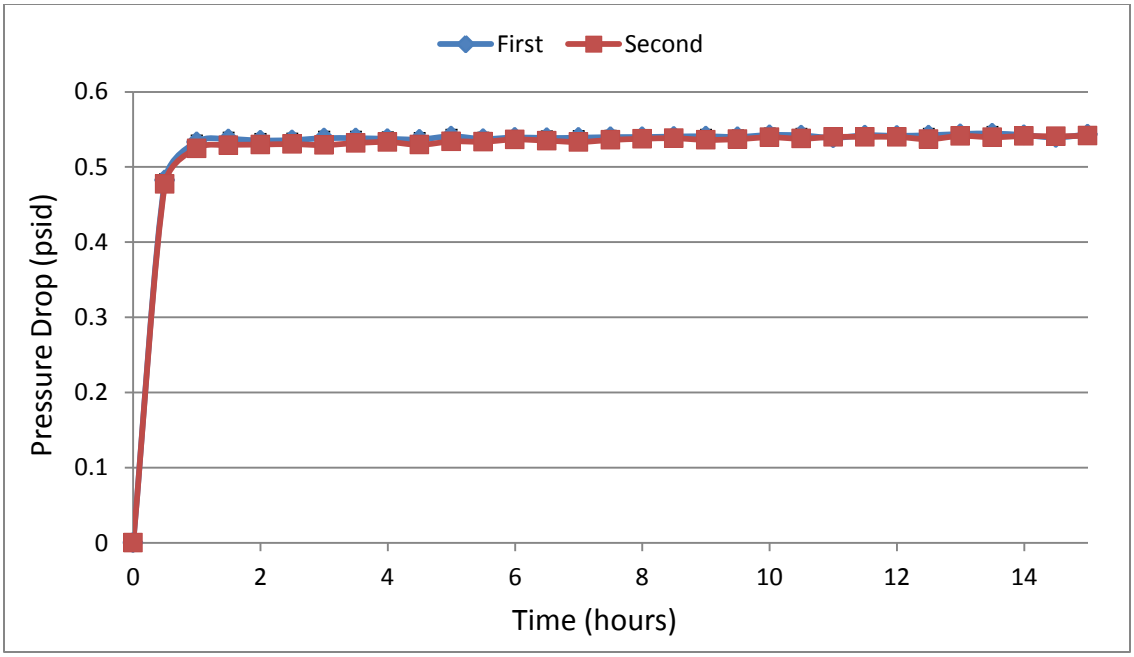

Figure 6.30 Head Loss Data (Vogtle Strainer, STDEV ±1.61%, 3.112 cm/s, 40g)

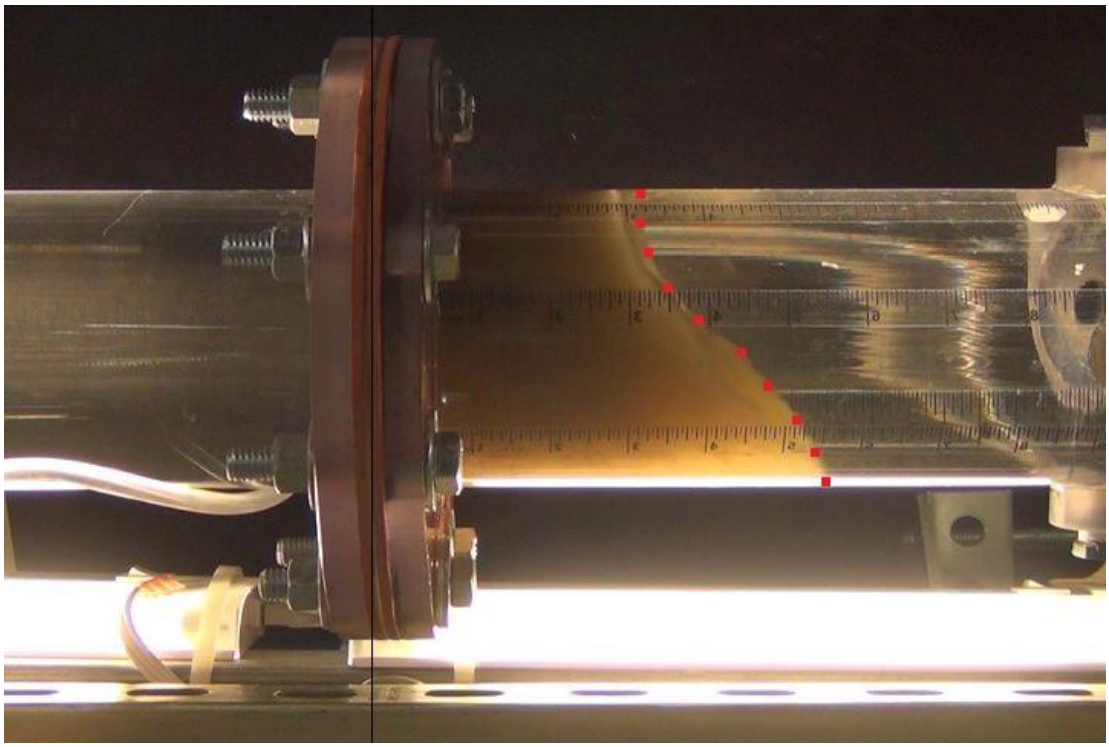

Figure 6.31 Final Debris Bed Thickness (Vogtle Strainer, 3.112 cm/s, 40g)

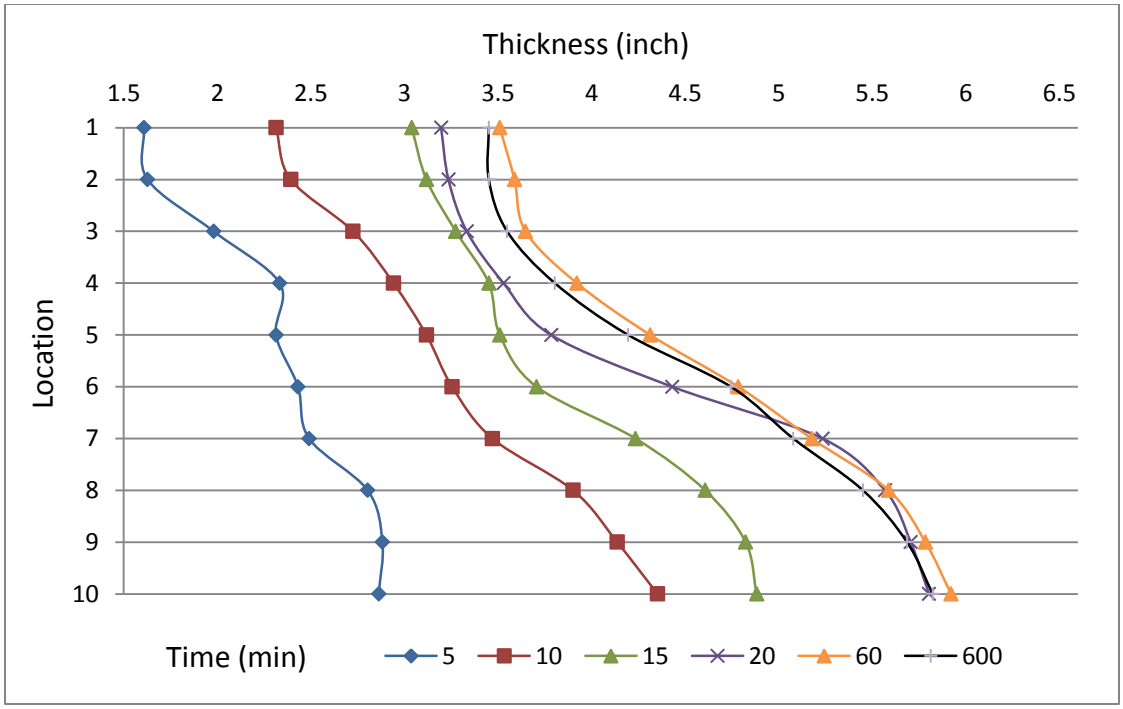

Figure 6.32 Debris Bed Buildup over Time (Vogtle Strainer, 3.112 cm/s, 40g)

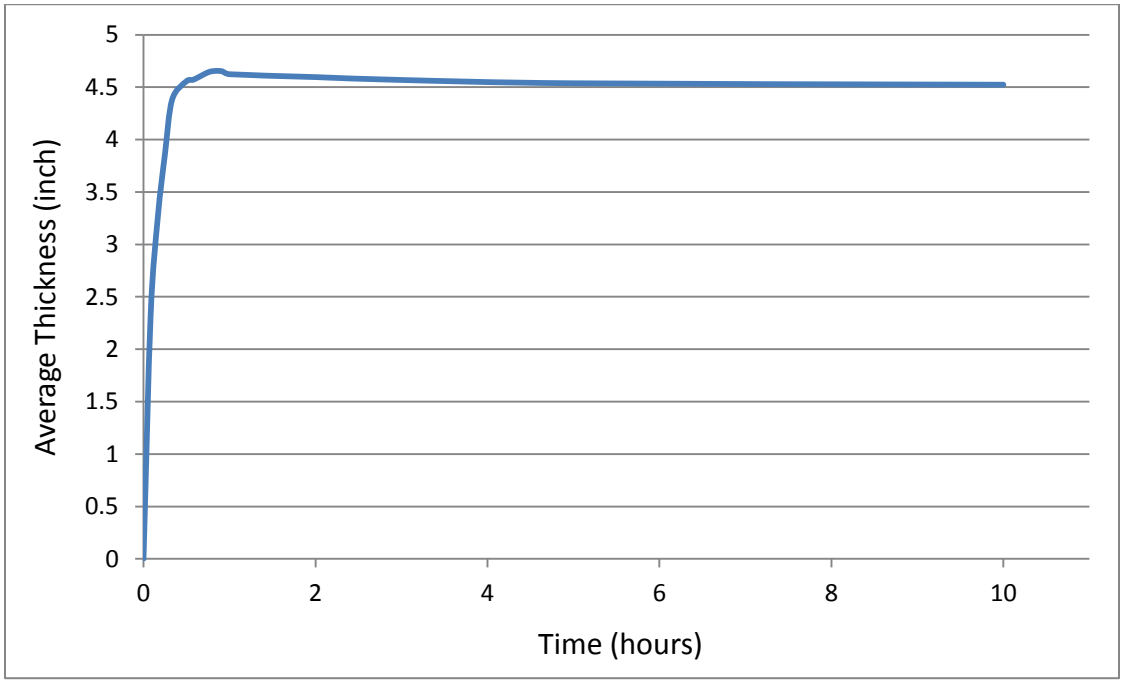

Figure 6.33 Debris Bed Thickness over Time (Vogtle Strainer, 3.112 cm/s, 40g)

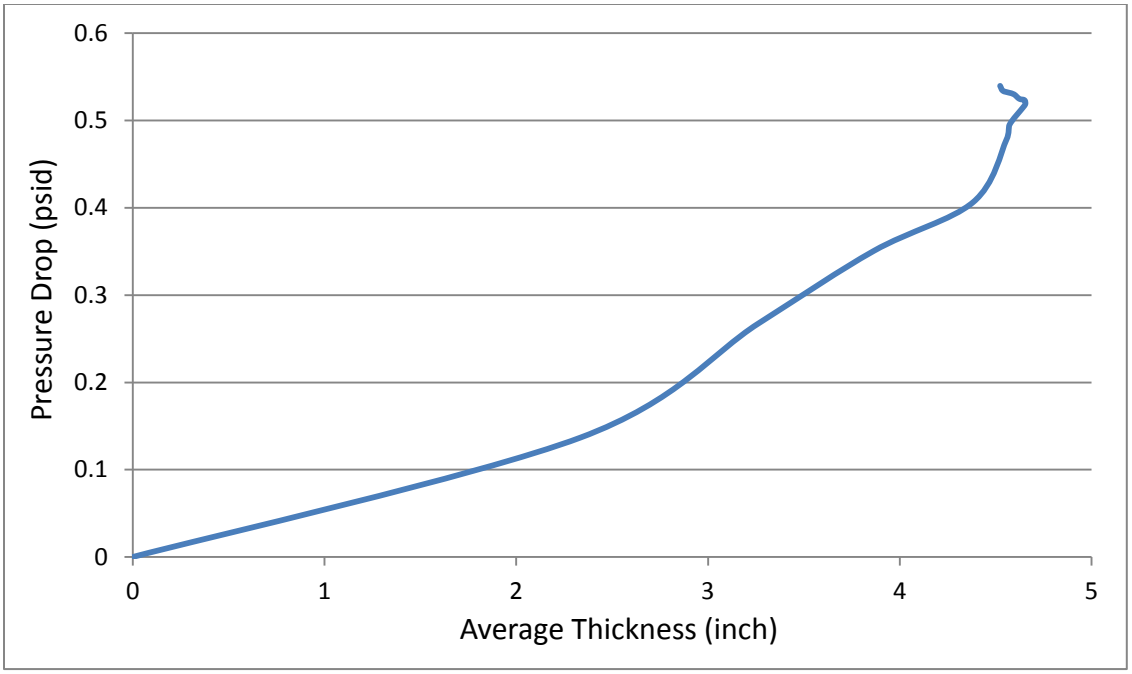

Figure 6.34 Pressure Drop as a Function of Thickness (Vogtle, 3.112 cm/s)

6.2.4 Comparison and Discussion

One test for each approaching velocity was analyzed by calculating the average bed thickness at designated time intervals using the 10 pints method. For each selected time interval, the pressure drop corresponding to that time interval was calculated by averaging the pressure drop values for 10 second before and 10 seconds after the designated time. The calculated pressure drop was plotted against time for each approaching velocity as shown in Figure 6.35.

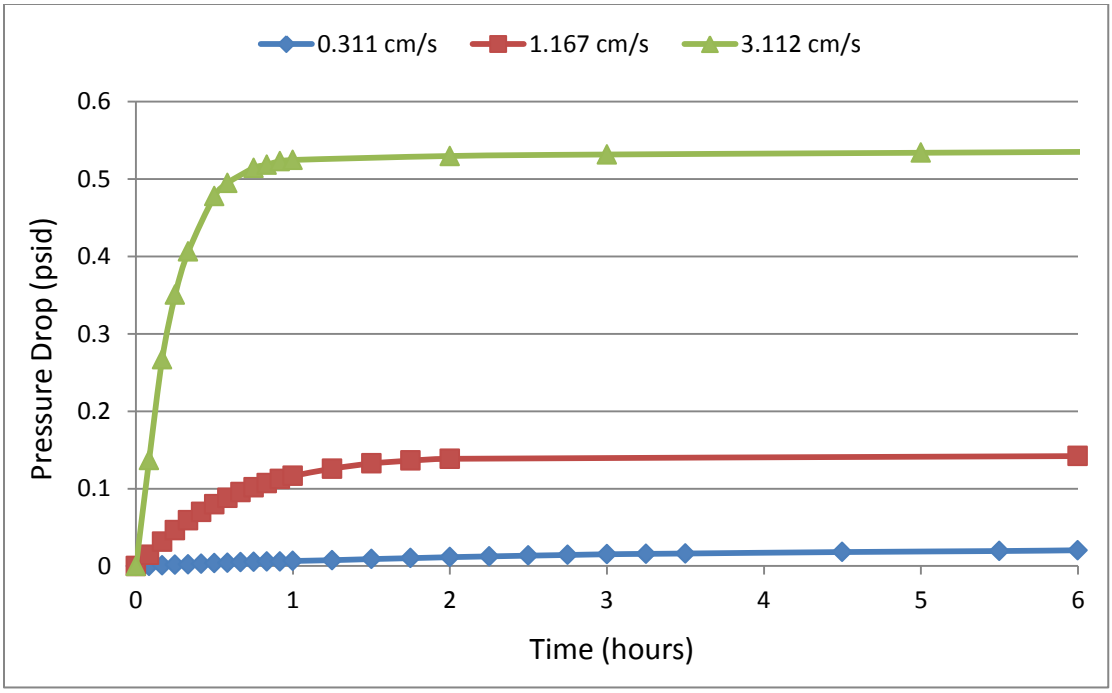

Figure 6.35 Pressure Drop at Different Approaching Velocities (Vogtle Results)

The steady sate pressure drop for the minimum approaching velocity (0.311 cm/s) was about 0.0241 psid on average, and the pressure drop for the Intermediate range (1.167 cm/s) was about 0.1477 psid on average, which is more than six times higher than the head loss for the minimum range. The pressure drop for the maximum range (3.112 cm/s) was about 0.546 psid, which is almost four times higher than the intermediate range and a more than 22 times the minimum range. The final average bed thickness for the minimum approaching velocity was larger than 11.34 inch, The final debris bed for the intermediate range was about 7.54 inch, which is about 33% less than the minimum range. The final average debris bed for the maximum range was about 4.53 inch, which is about 40% less than the intermediate range and 60% less than the

minimum range. The average bed thickness for each test was plotted against time and compared to each other as shown in Figure 6.36. The pressure drop was plotted as a function of the average bed thickness to study the effect of the flow rate on the debris bed thickness. It was observed that higher flow rates affected the shape of the debris bed and increased the head loss due to the compression of the debris bed that caused by the liquid inertia, which in turn, effect other parameter such as volume, density and porosity. For higher approaching velocities, the pressure drop and the debris bed thickness have a non-linear relationship as shown in Figure 6.37.

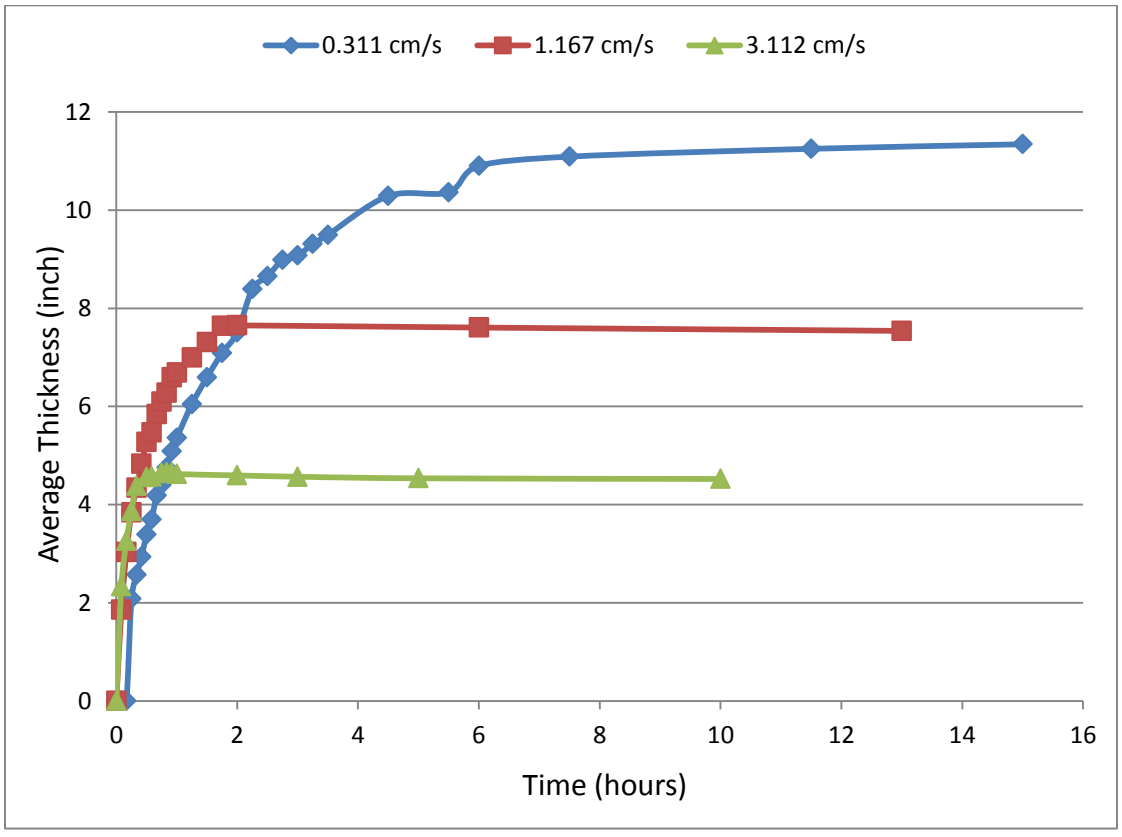

Figure 6.36 Average Debris Bed Thickness over Time (Vogtle Results)

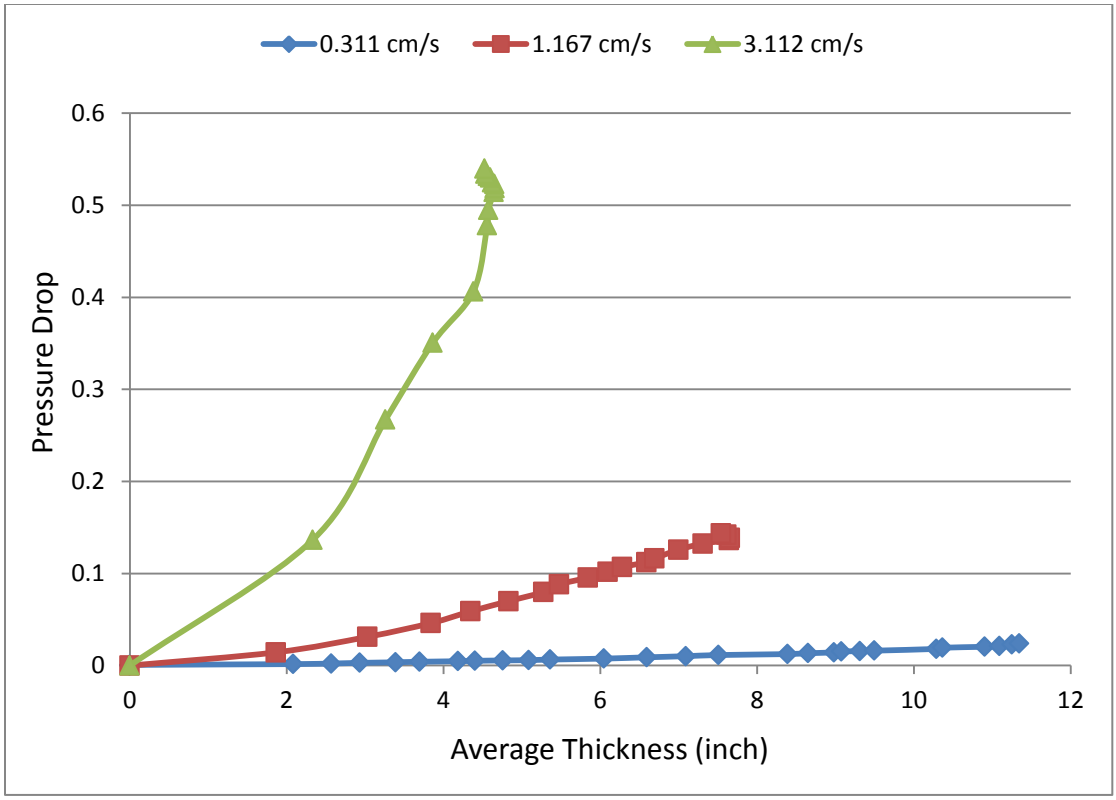

Figure 6.37 Pressure Drop as a Function of Thickness (Vogtle Results)

6.3 NUKON Mats

All the tests for the STP strainer were conducted using the same NUKON mat (Mat #1, Lot# 10958HT) while, all the tests for the Vogtle strainer were performed using another NUKON mat (Mat #2, Lot# J-148-12HT,). The two mats have the same properties and characteristics and are identical (according to the manufactured company). A preliminary study was performed to investigate the difference between the two mats by performing a few tests with the same conditions. The experiment were performed for the intermediate range as shown in Figure 6.38, and for the maximum range as shown in Figure 6.39.

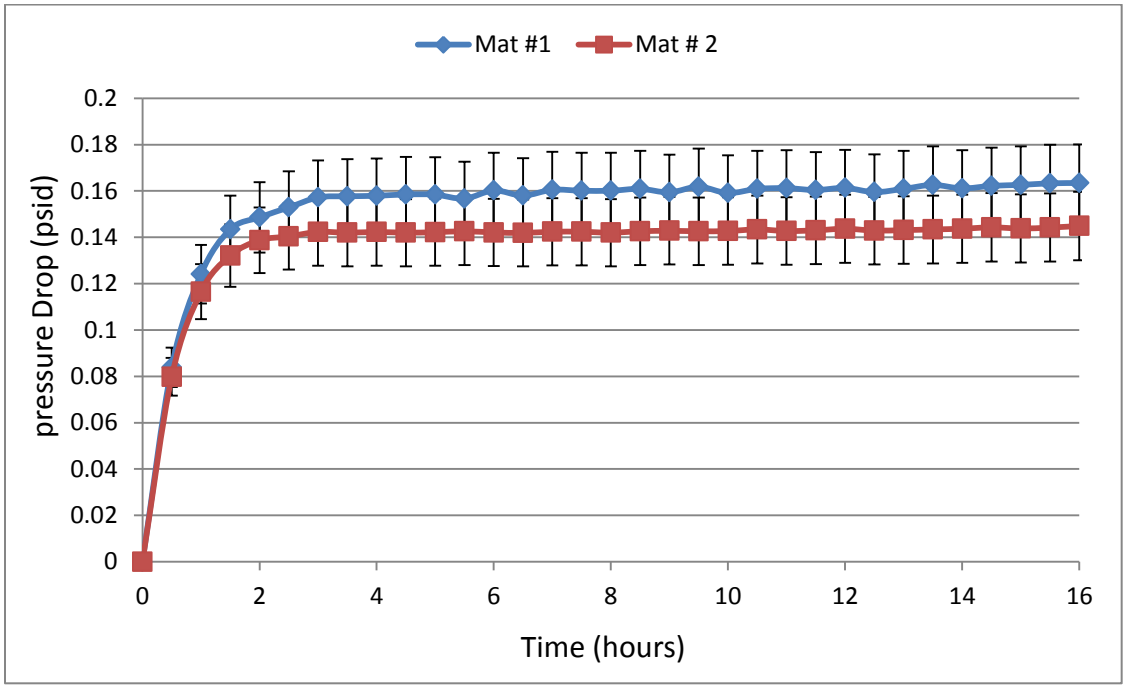

Figure 6.38 Head Loss by Different NUKON Mats (STDEV ±10.2%, 1.167 cm/s)

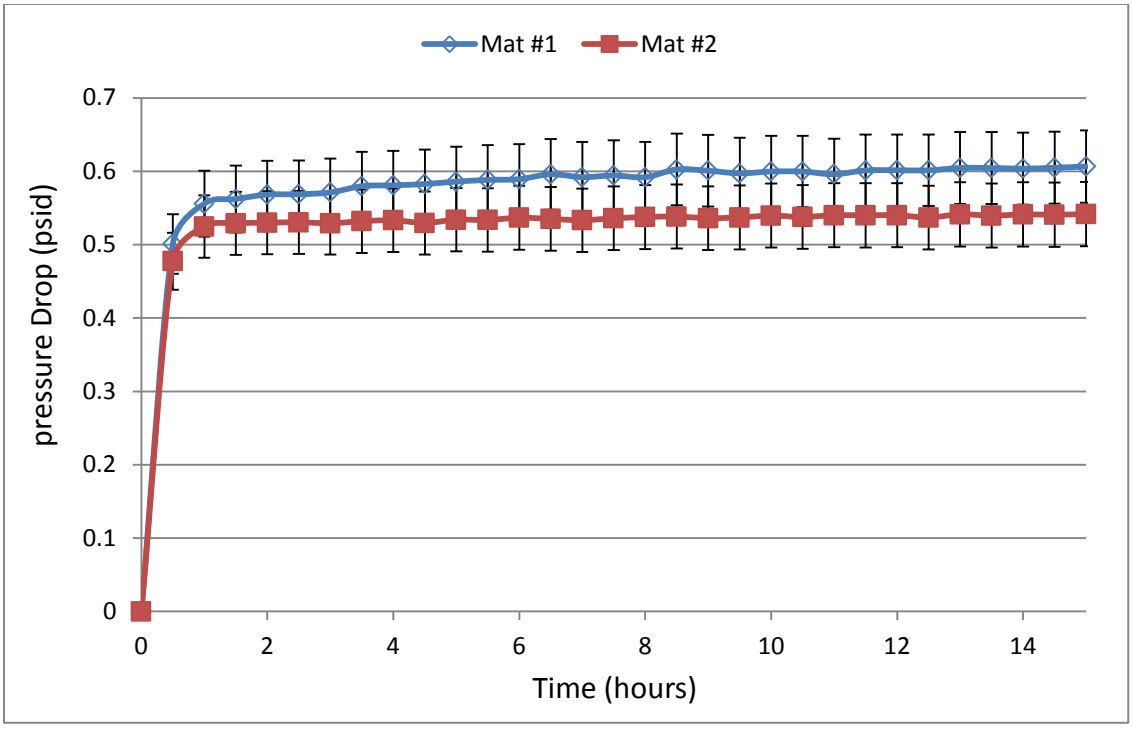

Figure 6.39 Head Loss by Different NUKON Mats (STDEV ±8.1%, 3.112 cm/s)

It was observed that the pressure drop from the old NUKON mat (Mat #1) was Always higher than the pressure drop from the new NUKON mat (Mat#2). For the intermediate range the pressure drop was 0.161 psid for the old mat and 0.144 psid for the new mat, which is 10.5% less. For the maximum range the pressure drop for the old mat was 0.591 psid and 0.540 for the new mat which is 8.6% lower. We can conclude that, the two NUKON mats have slightly different properties, yet, not a significant difference. The difference between the two mats is within the range of the tests results the uncertainty and can be neglected for this experimental condition.

6.4 Strainers Comparison

The difference between tests results from the two strainers was investigated in order to determine the significance of the difference, if any. The two strainers were compared based on the pressure drop as shown in Figure 6.40 for the minimum range, Figure 6.41 for the intermediate range, and Figure 6.43. Since the error bars from the two test overlap, we can conclude that there is no significant difference in the pressure drop between the two strainers and the difference can be neglected for the minimum approaching velocity.

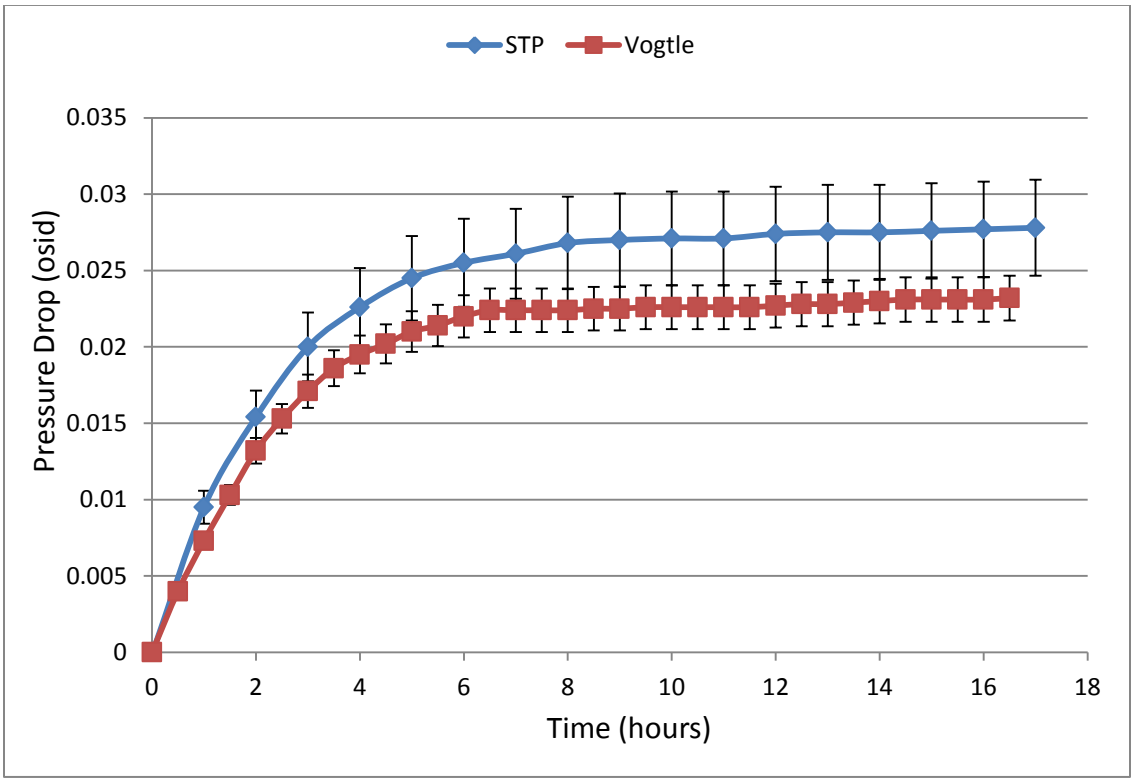

Figure 6.40 Head Loss Data (STP versus Vogtle, 0.311 cm/s, 40g)

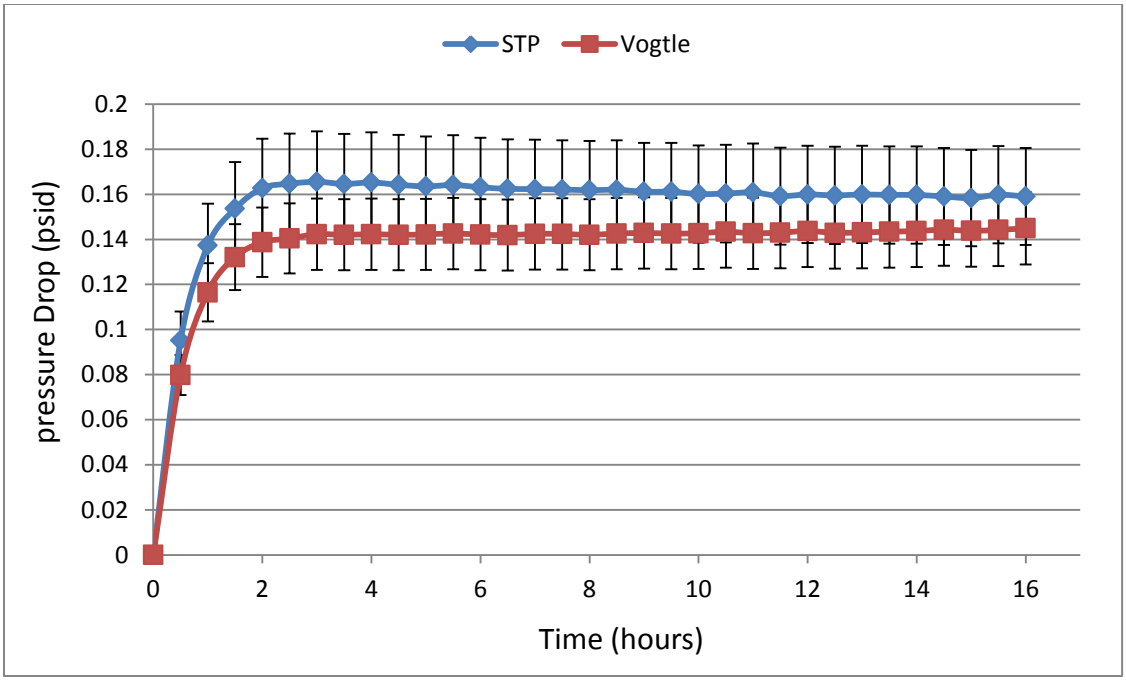

Figure 6.41 Head Loss Data (STP versus Vogtle, 1.167 cm/s, 40g)

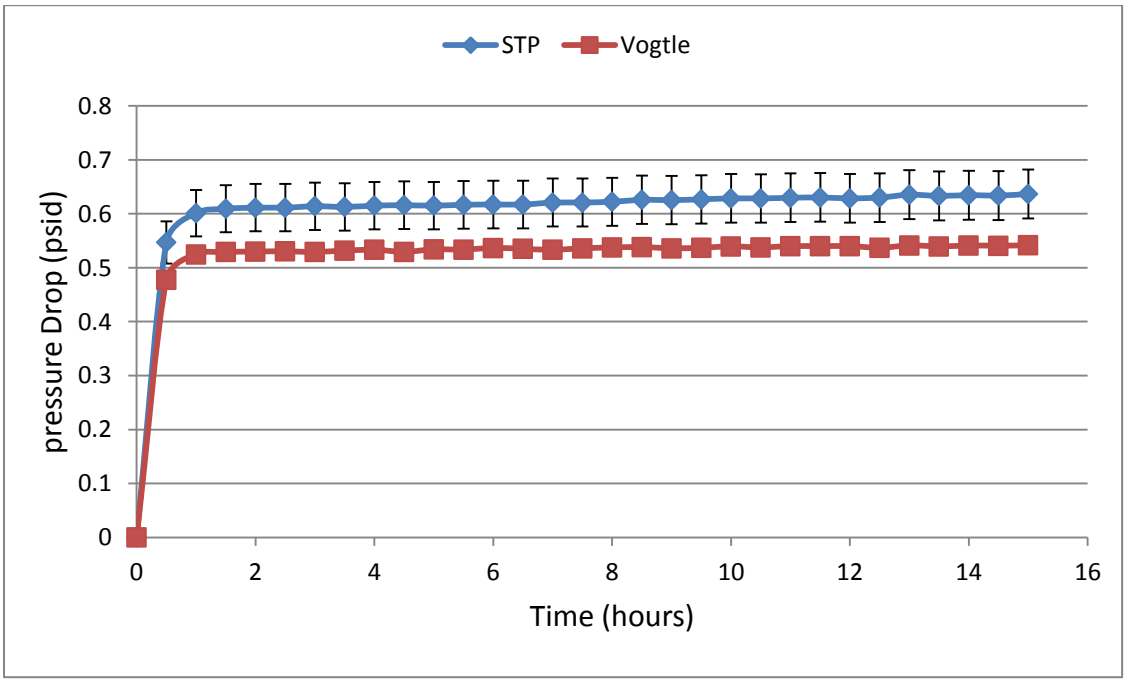

Figure 6.42 Head Loss Data (STP versus Vogtle, 3.112 cm/s, 40g)

We can have the same conclusion for the intermediate approaching velocity, the error bars overlap, thus, the difference between the two strainers is insignificant for this range. For the maximum approaching velocity the error bars don't overlap and the steady state pressure drop for the STP strainer is 0.637 (±7.17%) psid, and for the Vogtle strainer is 0.542 (±1.16%), which means there is ±17.5 % difference, the difference was further investigated to determine its significance. This difference can be caused by the flow rate measurement uncertainty, the viscosity difference, the density difference, and the porosity difference. The flow meter accuracy was ±5% and it was observed that for the maximum range, the approaching velocity at the end of the test is 5% less than the beginning of the test, thus, it was determine that the total flow rate measurement uncertainty is less than 10%. Equation 2.2 (section 2) was used to calculate the difference in the pressure drop measurement due to these uncertainties after calculating the Kozeny constant coefficients. In order to calculate the Kozeny constant coefficients, a permeability model was developed for related experimental study condition, the calculated values of the Kozeny coefficients were then used to calculate the pressure difference using equation 2.2.

7. ANALYSES

The objective of this study was to suggest a realistic permeability model for the NUKON fiber glass insulation material, as mentioned before, which can be utilized in related applications. After investigating the head loss across the debris bed due to the accumulation of NUKON debris on the sump strainers, the results were employed to develop a permeability model, and to calculate the Kozeny constant coefficients, *a* and *b*. In order to calculate these coefficients, we needed to calculate the porosity using equation 2.4, the porosity was calculated based on the mass of the debris bed on the strainer M_S, average bed thickness $L_{avg.}$, and the density of the NUKON bed. The porosity can be calculated from Equation 7.1,

$$\varepsilon = 1 - \Phi \tag{7.1}$$

where, Φ is the solidity, which can be defined in Equation 7.2,

$$\Phi = \frac{V_N(t)}{V_B(t)} \tag{7.2}$$

where, V_N is the volume of the NUKON Particle and V_B is the volume of the NUKON debris bed as defined in Equation 7.3,

$$V_B(t) = A\, L_{avg.}(t) \tag{7.3}$$

where, A is the surface area of the debris bed, same as strainer, and $L_{avg.}$ is the average debris bed thickness. The average debris bed thickness, L_{avg}, was calculated at any time interval using the 10 points method. The volume of the NUKIN particle, V_N, was simply calculated from equation 7.4,

$$V_N = \frac{M_S(t)}{\rho_N} \tag{7.4}$$

where, M_S is mass of the NUKON on the strainer, it was calculated from Equation 7.5,

$$M_S(t) = M_{T_0} - M_T(t) \tag{7.5}$$

where, M_T is the mass of the debris in the tank as defined in Equation 7.6,

$$M_T(t) = C_T(t)\, V_T \tag{7.6}$$

where, C_T is the concentration of the debris in the tank, and V_T is the volume of the tank, the change of the debris mass in the tank is shown in Equation 7.7,

$$\Delta M_T(t) = M_{T_{in}} - M_{T_{out}} \quad 7.7$$

Once the debris leave the tank, they accumulate on the strainer surface forming the debris bed, thus, M_{Tin}, the mass of the debris entering the tank is equal to zero. After plugging equation 7.6 into equation 7.7, and take the derivative we get Equation 7.8,

$$\frac{dC_T(t)V_T}{dt} = -C_T(t)A\,U \quad 7.8$$

The last equation cab be re-organized as shown in Equation 7.9,

$$\frac{dC_T(t)}{C_T} = -\frac{A\,U}{V_T}dt \quad 7.9$$

After some algebra, the later equation can be re-written as shown in Equation 7.10,

$$C_T = e^{-\frac{A\,U\,t}{V_T}+C} \quad 7.10$$

The above equations were used to calculate the mass of the debris in thank using equation 2.5 in order to calculate the porosity (from equation 2.4, section 2). The results from these calculations were used to plot the porosity as a function of the average debris bed thickness (Figures 7.1 and 7.2).

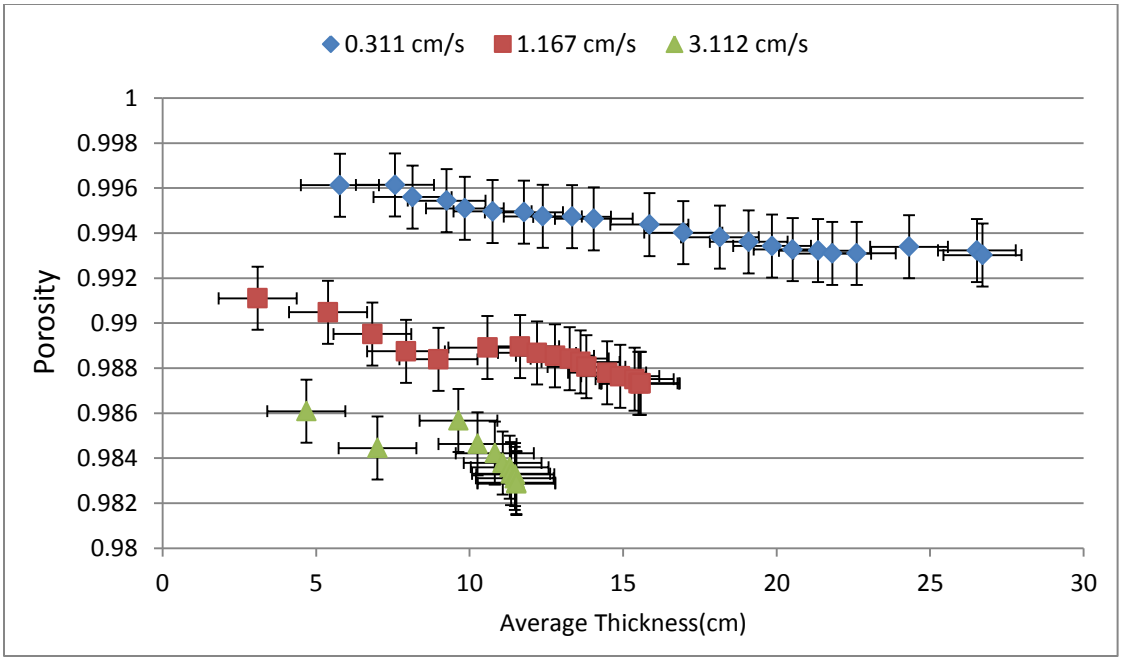

Figure 7.1 Porosity as a Function of the Debris Bed Thickness (STP)

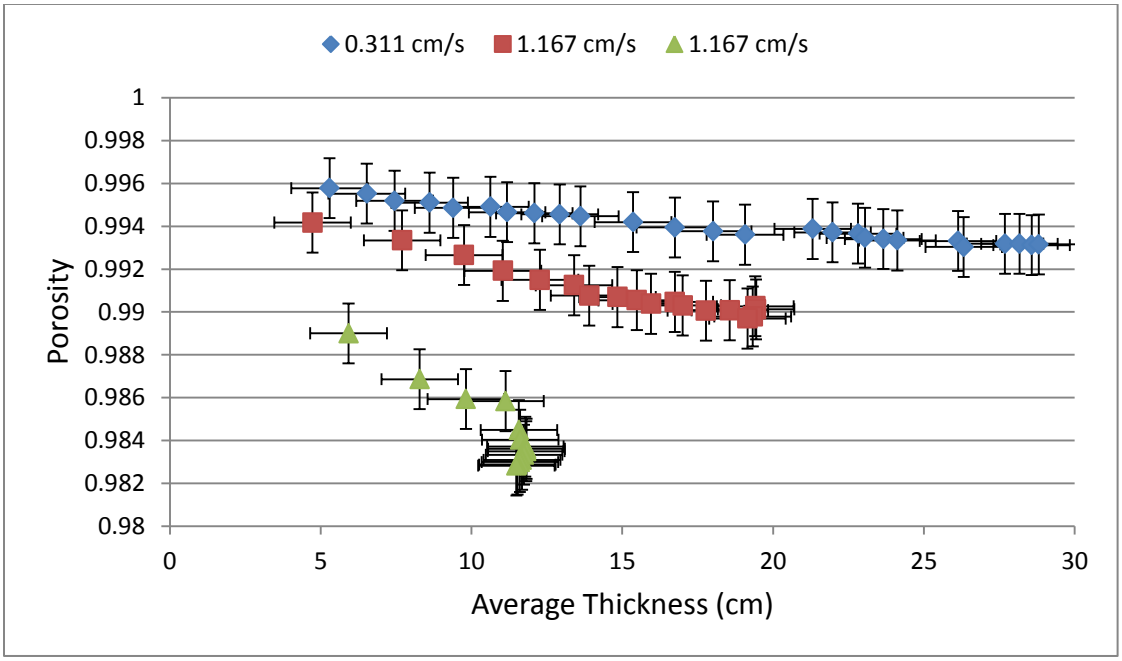

Figure 7.2 Porosity as a Function of the Debris Bed Thickness (Vogtle)

For the minimum approaching velocity, the final debris bed was thicker than the intermediate range with higher porosity. For the intermediate range the debris bed thickness was less than the minimum range and higher than the maximum range, while, it has less porosity than the minimum range and higher porosity than the maximum range (Figure7.1 and 7.2). Since only the minimum range of the approaching velocity is in the viscous flow regime, based on the modified Reynolds number, only the data from the minimum approaching velocity test were used to calculate the permeability, K, and Kozeny constant, k, as shown in Table 7.1.

Table 7.1 Permeability and Kozeny Constant of Fibrous Porous Media

Author	ε	$K\ (m^2)$	k
Present Study (STP strainer)	0.993	4.6×10^{-9}	14.2
	0.995	7.3×10^{-9}	17.7
Present Study (Vogtle strainer)	0.993	4.9×10^{-9}	13.5
	0.993	9.8×10^{-9}	13.3
Davis	0.99	N/A	27.6
Ingmanson et al.	0.9884	N/A	31.4

The experimental data from this study was best described by the present permeability model developed for related experimental work. The present model suggested new coefficients for to modify Davies correlation (equation 2.3).

The values of the coefficients *a* and *b* were suggested to be 1.9 and 125 respectively, the suggested permeability model is shown in Equation 7.11,

$$k = \mathbf{1.9}\frac{\varepsilon^3}{(1-\varepsilon)^{0.5}}[1 + \mathbf{125}(1-\varepsilon)^3] \qquad 7.11$$

The coefficient, *a* and *b*, were used in equation 2.4 to calculate the pressure drop difference for the maximum range approaching velocity to determine the significance of the flow measurement uncertainty. The experimental values of the pressure drop were 0.637 for STP and 0.542 for Vogtle, the difference between the two strainers was ±17.5%. The calculated values of the pressure drop, using equation 2.4, were 0.764 psid for the STP strainer and 0.732 psid for the Vogtle strainer, the difference between the two strainers was ±4.5%. All the test in this experimental study were performed under controlled room temperature 24±3º C, the temperature effect on the viscosity and the density of the water was investigated. The viscosity of water was 8.856E-4 (Pa.s) at 24º C and 8.300E-4 (Pa.s) at 27º C, the difference between the two viscosities is ±6.75%. The density of water was 9.968E+2(kg/m^3) at 24º C and 9.961E+2 (kg/m^3) at 27º C, the difference in the density was less ±0.07% which is negligible. Since the calculated values of the pressure drop had lower difference than the experimental values, it means that the flow rate measurement uncertainty was the main reason for this difference. There is a probability that the debris bypass could be different between the two strainers, thus, a debris bypass study is required to further investigate this difference.

The experimental pressure drop values for the two strainers were compared to the pressure drop values calculated from the NUREG-6224 model (equation 2.4) and the values calculated from the present model as shown in Table 7.2. The pressure drop values predicted by the present model showed better agreement with the experimental data from the NUREG-6224 model.

Table 7.2 Pressure Drop Values Comparison

	Pressure Drop (psid)		
Strainer Type	Experiment	NUREG-6224	Present model
STP	0.637 psid	1.255	0.764
Vogtle	0.542 psid	1.257	0.732

8. CONCLUSION

Two types of perforated plates were installed vertically in a flow loop to measure the head loss through the fibrous debris bed accumulated on the strainer. The head loss was measured at three different approaching velocities with a designated quantity of NUKON insulation material. The accumulated debris bed thickness was calculated at different time intervals for each case, and the characteristics of the debris bed were investigated. The tests results were compared with each other based on the approaching velocity, debris bed thickness, and strainer type. A realistic permeability model was suggested based on related experimental studies. The permeability model was developed from experimental data acquired from approaching velocities in the viscous region. There was no significant head loss difference between the two strainers for the minimum and intermediate approaching velocities. The Vogtle strainer had lower pressure drop than the STP strainer, but they both had the same bed thickness. The head loss difference between the two strainers for the maximum range was ±17.5% which is about four times higher than the calculated pressure drop. The calculated values of the pressure drop had lower difference than the experimental values, meaning that, the flow rate measurement uncertainty was the main reason for this difference. There is a probability that the debris bypass could be different between the two strainers, thus, a debris bypass study is required to further investigate this difference.

REFERENCES

1. U.S. Nuclear Regulatory Commission, "Power Reactors," NRC.gov, Washington, D.C., December 13, 2013.
2. M. R. Fard, "Assessment of Debris Accumulation on PWR Sump Performance," U.S. Nuclear Regulatory Commission, NUREG-0933, Rev.2, Main Report with Supplements 1-34, Washington, D.C., March 29, 2012.
3. A. W. Serkiz, "Containment Emergency Sump Performance," U.S Nuclear Regulatory Commission, NUREG-0897, Rev.1, Washington, D.C., October 1985.
4. U.S Nuclear Regulatory Commission, "Potential Impact of Debris Blockage on Emergency Recirculation during Design Basis Accidents at Pressurized-Water Reactors," Generic Letter (GL 2004-02), Washington, D.C., September 13, 2004.
5. C.J. Shaffer, D.V. Rao, M.T. Leonard, K.W. Ross, "Knowledge Base for the Effect of Debris on Pressurized Water Reactor Emergency Core Cooling Sump Performance," U.S. Nuclear Regulatory Commission, NUREG/CR-6808, 2003.
6. D. V. Rao, E. J. Souto, "Experimental Study of Head Loss and Filtration for LOCA Debris," U.S. Nuclear Regulatory Commission, NUREG-CR-6376, Washington, D.C., 1996.
7. P. C. Carman, "Flow of Gases through Porous Media," Academic Press INC., London, 1956.

8. W. L. Ingmanson, B. D. Andrews, and R. C. Johnson, "Internal Pressure Distribution in Compressible Mats under Fluid Stress," TAPI Journal, Vol.42, Issue 10, 1959.
9. S. Ergun, “Fluid Flow through Packed Columns” Chemical Engineering Progress, Vol. 48, Issue 2, 1952.
10. G. Zigler, J. Brideau , D. V. Rao, C. Shaffer, E. Souto, W. Thornas, “Parametric Study of the Potential for BWR ECCS Strainer Blockage Due to LOCA-Generated Debris,” U.S Nuclear Regulatory Commission, NUREG/cr-6224, Final Report, Washington, D.C., October 1995.
11. C. N. Davies, “The Separation of Airborne Dust and Particles,” Proceedings of the Institution of Mechanical Engineering, London, 1952.
12. B. Letellier, “Risk-Informed Resolution of GSI-191 at South Texas Project. Technical Report,” South Texas Project, Rev. 0, Texas, 2011.
13. T. D. Sande, B. C. Letellier, G. L. Zigler “CASA Grande Analysis,” South Texas Project Risk Informed GSI-191 Evaluation, Technical Report , Rev.2, Volume 3, Texas, November 6, 2013.
14. Performance Contracting Inc. “NUKON® Insulation Material Safety Data Sheet,” No. MSDS 05, Rev. 7, Kansas, January 22, 2007.
15. W.W. Grainger Inc., “Grainger Catalog,” Catalog 405, Multifunction Time-delay, Dayton Model# 1EJE9, Global Company, 2014.
16. Honeywell International Inc., “Ultra Precision Wet/Wet Differential Pressure Transducer,” Model # TJE, May 2008.

17. KTOHNE Messtechink GmbH, “OPTISONIC 6400 Handbook,” Portable Ultrasonic Clamp-on Flowmeter, Electric Revision (ER 1.1.0), SW.REV 01.01.01, Duisburg, Germany, August 2011.
18. King Instrument Company, “King Catalog,” Version D600, California, March 2013.
19. Honeywell International Inc., “ SC series Instruction Manual,” SC Instrumentation, Sensing and Control, Signal Conditioning Self-Calibrating Digital Indicators, Document # 008-0608-00, Ohio, 2005.
20. Sony Corporation, “Digital HD Video Camera recorder handbook,” Model HDR-XR260, Japan, 2012.
21. Nuclear Energy Institute, “ZOI Fibrous Debris Preparation: Processing, Storage and Handling,” Rev. 1, Washington, D.C., January 2012.
22. Clean Force Power Washer Company, “Electric Powered High Pressure Washer Operating Manual,” Model# CF1800HD, Ver. 3, Sumec North America, Texas.